An-Najah National University

Faculty of Graduate Studies

Efficiency of Magnetic $CoFe_2O_4$ Supported on Graphene for Removal of Cyanide from Wastewater

By

Ahmad Khader Taha Zubaida

Supervisor

Prof. Shehdeh Jodeh

This Thesis is Submitted in Partial Fulfillment of the Requirements for the Degree of Master of Chemistry, Faculty of Graduate Studies, An- Najah National University, Nablus-Palestine.

2018

Efficiency of Magnetic $CoFe_2O_4$ Supported on Graphene for Removal of Cyanide from Wastewater

By

Ahmad Khader Taha Zubaida

This Thesis was defended successfully on 19/6/ 2018, and approved by:

Defense Committee Members	**Signature**
Dr. Shehdeh Jodeh /Supervisor	…………………………………..
Dr. Subhi Samhan / External Examiner	…………………………………..
Dr. Ahed Zyoud / Internal Examiner	…………………………………..

Dedication

Every challenging work needs self-efforts as well as encouragements of others especially those who are very close to our heart.

To my father, And my dear family whose love and encouragement make me able to get success and honor. My great mother who sacrificed for our sake.

To all of them I dedicate my modest efforts.

Acknowledgements

In the beginnings, praise and thank to Allah Almighty, who gave me the ability to complete this work, without his help my effort would have gone astray.

Special thanks to my research supervisor Prof. Dr. Shehdeh Jodeh for giving me the opportunity to work with their research group. I would also to thank the defense committee members : Dr. Subhi Samhan and Dr. Ahed Zeyod for their patience to read my thesis and provide useful suggestions.

Many thanks to Middle East Desalination Research Center (MEDRC) who funded my project through the Palestinian Water Authority whom our thanks go as well to them for their follow up the project.

To all in Chemistry Department at An-Najah National University I offer my honest gratitude, in particular laboratory technician Mr. Nafiz Dweikat. To my colleagues, my supporters, and my friends, I offer my sincere thanks.

Finally, I would like to thank Mr. Carlos Adelantado from university of Castilla La Mancha in Spain for helping Prof. Dr. Jodeh for the sample synthesis and preparation. Also, many thanks goes to Prof. Manuel Algarra from University of Malaga in Spain for doing sample characterization.

الإقرار

انا الموقع ادناه مقدم الرسالة التي تحمل العنوان:

Efficiency of Magnetic $CoFe_2O_4$ Supported on Graphene for Removal of Cyanide from Wastewater

أقر بأن ما اشتملت عليه هذه الرسالة إنما هي نتاج جهدي الخاص، باستثناء ما تمت الإشارة إليه حيثما ورد، وأن هذه الرسالة ككل، أو أي جزء منها لم يُقدم لنيل أية درجة أو لقب علمي أو بحثي لدى أي مؤسسة تعليمية أو بحثية أخرى.

Declaration

The work provided in this thesis, unless otherwise referenced, is the researcher's own work, and has not been submitted elsewhere for any other degree or qualification.

Student's Name:	**اسم الطالب:**
Signature:	**التوقيع:**
Date:	**التاريخ:**

Table of contents

List of Tables

List of Figures

List of Abbreviation

Symbol	Abbrevia
A°	Angstrom = 1.0 × 10^{-10} meters
A_o	absorbance of cyanide in the sample solution before treatment
Abs.	Absorbance
A_e	Absorbance of cyanide in the sample solution after treatment
ARIJ	Applied Research Institute Jerusalem
B	Dimensionless Temkin constant
BOD	Biological Oxygen Demand
COD	Chemical Oxygen Demand
C_o	Concentration of cyanide in the sample solution before treatment (mg/L)
C_e	Concentration of cyanide in the sample solution after treatment (mg/L) at equilibrium
C_i	Initial concentration of cyanide in the sample solution (mg/L)
DSC	Differential scanning calorimetry
EQA	European Quality Assurance
FT-IR	Fourier Transform Infrared
IQ	Intelligence Quotient
K_1	The Lagergren's first order rate constant
K_2	The pseudo second order rate constant
K_d	The distribution coefficient
K_F	Freundlich constant which is an approximate indicator of adsorption capacity of the sorbent (mg/g $(L/mg)^{1/n}$)
K_L	Langmuir isotherm constant (L/mg)
MAC	Minimum alveolar concentration
LD50	Lethal Dose which causes the death of 50% (one half) of a group of test.
MAO-A	Monoamine oxidase A
MAOI	Monoamine oxidase inhibitors
CN^-	Cyanide
MAD	Mass of adsorbent dose

N	Dimensionless Freundlich constant giving an indication of how favorable the adsorption process
OPT	Occupied Palestinian territories
PCBS	Palestinian Central Bureau of Statistics
Qe	The amount of CN adsorbed per gram of the adsorbent (mg/g)
Qm	Maximum monolayer coverage capacity (mg/g)
Qt	Amount of adsorbate per unit mass of adsorbent at time t (min)
R	The gas constant (8.314 J/mol K)
R2	Correlation coefficient (regression coefficient)
RL	Dimensionless constant separation factor
SEM	Scanning Electron Microscope
$G\text{-}Cofe_2O_4$	Graphene cobalt ferrite
MGONH	Magnetic graphene oxide Nanohybride
SPE	Solid Phase Extraction
SVR	Systemic Vascular Resistance
t	Time
T	The absolute temperature (Ko)
TGA	Thermal Gravimetric Analysis
V	Volume of Solution
ΔG°	Stander Gibbs Energy
ΔH°	Standard Enthalpy
ΔS°	Standard Entropy

Efficiency of Magnetic $CoFe_2O_4$ Supported on Graphene for Removal of Cyanide from Wastewater

By

Ahmad Khader Taha Zubaida

Supervisor

Prof. Shehdeh Jodeh

Abstract

There are many contaminants that seep into soil and groundwater from untreated wastewater discharched to open environment, So it causes many health problems for animals and environment, The main problem here is to detect the concentration of contaminants such as Cyanide and try to remove it by adsorption.

Produced Magnetic $CoFe_2O_4$ Graphene Oxide was characterized by several spectroscopic and analytical techniques SEM, TEM, XRD, FTIR VSM and TGA. SEM images of the magnetic showed rough and porous nature, indicating that the materials present good characteristics to be employed as an adsorbent. The adsorption experiments were conducted for a wide range of temperature, adsorbent dosage, pH, initial concentration and contact time. Result revealed that the cyanide is removed at a low temperature of 15 ° C and also in a acidic medium of 3 and the contact time after 25 and using a weight of 0.25 g of the initial dose and concentration of 15 mg / L of 50 mL CN solution. The removal efficiency of 91% of the Cyanide.

The adsorption of CN on the (M-$CoFe_2O_4$ / *GO*) was optimized under acidic conditions and temperatures 15 ^{O}C temperature. CN sorption using (M-$CoFe_2O_4$ / *GO*) can be described using pseudo second order and Langmuir isotherm model. Based on the results, the (M-$CoFe_2O_4$ / *GO*) is able to remove CN rapidly within 25 min with high removal efficiency.

The negative ΔG° values (-14.548to -12.595 KJ/mol) indicate that the adsorption is favorable and spontaneous at these temperatures. The negative value of ΔH° (-38.9 KJ/mol) reflects an exothermic adsorption and indicates that the adsorption is favored at temperature 15^{O}C. The value of ΔH° was higher than those corresponding to physical adsorption. The positive value of ΔS° (+83.14 J/mol.K) suggests that some structural changes occur on the adsorbent and the randomness at the solid/liquid interface in the adsorption system increases during the adsorption process.

Chapter One

Introduction

1.1 Overview

Cyanide is a very toxic compound that is released into the environment through the effluents of industrial activities such as metal plating, electronics, photography, coal coking, plastics, chemical fertilizer and mining. Cyanide is included in the priority list of hazardous substances and has adverse health effects on people as well as other living organisms. Exposure to small amounts of cyanide can be deadly irrespective of the route of exposure **[1].**

To make the aquatic life and earth cleaner make humans in a matter of importance, a subject of growing concern for the environment. Pollution caused by factors such as heavy metals and dyes from the list that made the environment invalid and a serious health concern for the population **[2].**

Of environmental pollutants Cyanide and toxicological agents of humans and aquatic organisms **[3]**. In the short term it is a strong inhibitor of breathing due to severe toxicity against cytochrome oxidase and is tightly bound to terminal oxides. Cyanide causes rapid breathing, tremors, and other neurological effects and affects the human body in the long run for weight loss, thyroid effects, nerve damage and death. Skin contact with fluids containing Cyanide may lead to irritation and ulcers. Cyanide can produce reasonable concentrations and occurs naturally when present in liquids (biogens from plants and microorganisms) and from human activities (waste from metallic coatings, raw filtration, production of synthetic fibers, plastics, pharmaceuticals, coal gas, mineral extraction, crop crops Cyanogens), which are the main source of natural water pollution by this compound **[4]**. Metal oxide adsorbents including iron, aluminum, manganese, titanium, and zirconium have underwent extensively investigation. Among which, iron oxides are the mostly studied due to their high affinity to cyanide species, low cost, and eco-friendly.Recently, considerable attention has been focused on the development of Fe-based binary sorbent **[5]**.

Various adsorbents, such as activated carbon, nanoparticles, biomaterials have been extensively applied for the removal of organic and inorganic pollutants from water and wastewater **[6]**. Among the various adsorbents, graphene oxide is one of the derivative of carbon family, which can be easily synthesized from the natural graphite using modified hummer's method. Graphene oxide contains more oxygen groups (such as AOH, ACOOH, AOA) and has abundant other functional groups, which help for higher adsorption of organic and inorganic pollutants **[7]**, due to increased number of active sites on their surface . Hence, more research is focused on using GO and their composites towards the removal of various pollutants **[8]**. There is easy stacking between layers due to p-p bonding between the GO layers while using for practical application. However, separation of GO from aqueous solution requires high energy centrifugation and separation techniques **[9]**. Hence, to overcome these drawbacks, functionalization of GO is one of the efficient way to increase the adsorption capacity of various pollutants **[10]**. To separate easily from the aqueous solution, magnetic nanoparticles are widely used as composite materials, attached with GO sheets, which can act as a magnetically recoverable adsorbent. Among the various magnetic materials, cobalt ferrite (CoFe2O4) nanoparticles have gained much attention, due to their high corrosive stability and moderate magnetic saturation, easy and rapid separation **[11]**. However, bare magnetic nanoparticles will aggregate to larger nanoparticles with fewer activating groups and will dissolve easily in acidic medium.

Water pollution with cyanide becomes a major concern around the world. The cyanide strength of metal ions makes it a favorable factor in electroplating, gold mining, and silver mining industries, thus producing a large amount of these industries **[12]**. Cyanide compounds in environmental matrices and waste flows can be classified as simple, complex cyanides and nitrides **[13]**. The most toxic form of cyanide is free cyanide, which contains the same anion cyanide and hydrogen cyanide (H), either in a gaseous or aquatic state. Sodium, potassium and calcium cyanide salts are very toxic, because they are very soluble in water, thus easily dissolving to form free cyanide.

At present, environmental pollution is measured by harmful and toxic compounds as one of the biggest problems in the world.

Industrial development has led to the elimination of harmful pollutants such as cyanide and its compounds in the atmosphere **[14]**. A large quantity of cyanide is disposed of various industries such as steel plant, textile, electroplating, petrochemicals and oil plants. Cyanide is toxic, carcinogenic, and mutagenic. Because of its many damaging effects, the elimination of cyanide from industrial wastewater early in its release into the water bodies is necessary **[15]**.

One of the traditional treatments for cyanide removal is in wastewater such as chemical electrochemical oxidation, solvent extraction, membrane separation and photolysis **[16]**. All these methods are expensive, time consuming and detailed. While adsorption is a very effective and more versatile method to eliminate all cyanide. Researchers have used Granular Activated Carbon (GAC) to dispose of cyanide from wastewater by absorption. Due to the high cost of this method is not suitable for developing countries, therefore, GAC has moved towards various types of low-cost biomaterials.

There has been a wide development in the secondary materials and for the absorption process new methods have been invented. Grafen (G), which emerges as new carbon materials with one-dimensional atom thickness, has shown great interest in the scientific environment due to the electrical, thermal and optical properties. To the high surface area. It is known that graphene and Graphene Oxide (GO) is a good condenser for many contaminants, but effective removal of water after treatment is still a challenge **[17]**.

It has been the use of magnetic fields in which they can be magnetic separation for the separation phase of the aqueous solutions, and to provide an easy and effective way in terms of cost for the practical operation of. Many efforts have been made to incorporate graphene and magnetic nanoparticles, because the new hybrid is also likely to possess Strengthen the functions with respect to adsorption **[18]**.

In the current work it has been reported approach to the preparation of $CoFe_2O_4$ magnetic grown on graphene layers using composite composite $CoFe_2O_4$-G separated magnetically from water. $CoFe_2O_4$ and $CoFe_2O_4$-G hybridized properties and a series of experimental parameters were analyzed systematically and optimally. Isotherm models, adsorption kinetics and thermodynamic properties were also studied to describe the adsorption process **[19]**.

The aim of this study is to remove Cyanide from wastewater, using this new prepared material as an adsorbent for the solid- phase extraction of cyanide. The adsorption behaviors of the new surface with cyanide will be studied. The effect of pH, temperature, and amount of adsorbent, concentration and the contact time on the adsorption of cyanide will be studied. The adsorption capacity will be investigated using kinetics and pH effects. Equilibrium Isotherm studies will be done by varying the following three parameters: initial concentration of cyanide solution, volume of the cyanide solution, and adsorbent dose on the uptake of cyanide from the solution.

1.2 Objective of this work

1.2.1 General Objectives

1. To remove Cyanide from wastewater, using this new prepared material as an Magnetic $CoFe_2O_4$ -Graphene Oxide .

2. To specify the optimal conditions for the adsorption

1.2.2 Specific objectives.

1. To determine if ($CoFe_2O_4$) can be used to clean up cyanide polluted wastewater.

2. To study the effect of pH, temperature, amount of adsorbent, concentration and contact time on the adsorption of cyanide.

Guideline and regulation trace metal and policy issue.

1.2.3 Research question and identified problems

The main questions addressed in this thesis are:

1. Can (GO-$CoFe_2O_4$) be used to remove Cyanide from wastewater?

2. To which extent that (GO-$CoFe_2O_4$) can improve efficiency Cyanide?

3. What are the optimum condition of pH, temperature, amount of adsorbent, concentration, and contact time for (GO-$CoFe_2O_4$) to adsorb Cyanide efficiently?

Chapter Two

Background and Literature review

2.1 Cyanide

2.1.1 Structure and Properties

Cyanide is present as anion form CN^- in some compounds such as Potassium Cyanide and Sodium Cyanide, which are highly toxic compounds , with IUPAC name **Cyanide** Because of the Cyanide anion of high nucleophilicity, cyano groups are introduced into organic molecules by displacement of a halide group.

Figure 2.1: Molecular structure scheme of the cyanide.

Chemical and Physical Properties of cyanide is summarized in Table 2.1 [20].

Table 2.1: Chemical and Physical Properties of potassium cyanide.

Physical and chemical properties	**Values**
Melting temperature	634.5C
Boiling temperature	1625
Solubility in water	71.6 g/100 ml (25 °C)
pka value	11.0
Molecular weight	65.12 g/mol
Color	White crystalline solid
Chemical formula	KCN

2.1.2 Uses of Cyanide

2.1.2.1 Industrial uses of Cyanide

Cyanide is found in many industries such as paints, papers and is present in low air emissions, Hydrogen Cyanide is used in the production of a number of chemicals and also as an insecticide [21]. Cyanide is mainly use for the mining of gold and silver, rubber, plastics, leather.

2.1.2.2 Medical Uses of Cyanide

Cyanide has more than one use as it is used as an expander in vascular research and cyanide is mainly a sodium nitroprocess compound in clinical chemistry to measure urinary ketone bodies mainly as a follow-up to diabetics.

Sometimes, it is used in emergency medical cases to produce rapid drop in blood pressure in humans. Cobalt in vitamin B12 artificial contains ligand cyanide as an artifact of purification process. This must be removed by the body before the vitamin molecule can be activated for biochemical use. During the First World War, copper cyanide compound was used in the treatment of tuberculosis and leprosy briefly by Japanese doctors [22].

2.1.3 Toxicity of cyanide

All cyanides are classified as hazardous material with acute and chronic characteristic of toxicity. Cyanide is highly toxic to humans and aquatic organisms [23]. It is a potent inhibitor of respiration due to its extreme toxicity towards cytochrome oxidase and by tightly binding to terminal oxidase. At short-term exposure, cyanide causes rapid breathing, tremors, and other neurological effects and long-term exposure to cyanide cause weight loss, thyroid effects, nerve damage and death. Skin contact with liquids containing cyanide may produce irritation and sores. The presence of cyanide in effluents can attain considerable concentrations and occurs both naturally (biogenes by plants and microorganisms) and from human activities (wastes from metal plating, ore leaching, production of synthetic fibers, plastics, pharmaceuticals, coal gasification, metal extraction and cyanogenic crop plants), which forms the major source of contamination of natural water by this compound.

Many Cyanides are highly toxic. Cyanic toxicity appears to be toxic hypoxia as anion cyanide is an inhibitor of cytochrome oxidase found in the mitochondrial membrane of eukaryotic cells. They attach to the iron inside this protein. The cyanide binding of this enzyme prevents the transfer of electrons from cytochrome to oxygen. As a result, the electron transmission chain has been disrupted, which means that the cell is no longer able to produce an antenna for power. [24] Tissues that rely heavily on aerobic respiration, such as the central nervous system and heart.

Table 2.2 shows the amount of cyanide dose and their respective effects on animals and humans

Table 2.2 Dose-related toxicity of Cyanide.

Animal studies	Toxic doses (ppm)	Manifestation
Rat	50	increased creatine phosphokinase
Monkey	100	severe dyspnea
Human studies	**Dose (mg/kg)**	**Toxic manifestations**
	546	Hemolytic anemia, skin desquamation in infants
	7	Nausea, vomiting, abdominal pain, chest pain, fever, hemolysis
	7.5	Hyperpyrexia, confusion
	20	Hypotension
	80	Bluish discoloration of skin (similar to cyanosis)

2.2 Cyanide in industrial effluents

A large number of Cyanide industries are produced annually worldwide, of which about 20-30% are wasted in industrial effluents during industrial processes and finishing.

Cyanide is widely used in paints, paper and medical treatments. The mining operations mostly use adsorbents for recovery and removal of cyanide from effluents. [25] Waste from these industries can affect our atmosphere, causing pollution. The level of contaminants even in a very low concentration is very obvious and will affect the aquatic life as well as the food network.

Approximately 15% of the world's total production of cyanide is lost and released into effluents. The release of contaminated water into the ecosystem is a serious source of pollution on human, plant and animal life, causing damage that can cause death [26].

The main symptoms of acute poisoning by cyanides are due to the interference of cyanide in the assimilation and distribution of oxygen in the body. Whether the cyanide source is HCN or ingestion of food containing a water soluble cyanide such as potassium or sodium salt, the poisoning mechanism is the same. The cyanide ions react irreversibly with the iron, in particular with the iron in the cytochrome c oxidase and hemoglobin. Since cyanides interfere with the absorption of oxygen and thus with the production of energy in the body, an increased exposure to cyanide will gradually show as headache, nausea, confusion, weakness, fatigue, loss of coordination, hyperventilation, cardiac arrhythmia, bradycardia, loss of consciousness and coma. Death typically occurs due to problems with the nervous system or the heart [27].

2.3 Industrial Wastewater in the Palestinian Territories

The absence of some basic tools in the management of hazardous waste in an inventory of hazardous national waste materials makes it difficult to determine which waste is being generated. Since there is no such stockpile in the Occupied Palestinian Territory and where it is disposed of. There are insufficient facilities for sewage treatment and treatment and disposal of wastewater in the Palestinian territories. There are very few estimates of the amounts of hazardous waste generated in the OPT. In the West Bank. Many other paint and other industries in the West Bank produce large quantities. Liquid wastes from these industries contain high concentrations of ionic materials and heavy metals. Annual solid and liquid hazardous waste estimates are 290 and 600 tons, respectively. It consumes large quantities of rare freshwater, generates and releases similar quantities of wastewater with large pollution loads, and sometimes with maximum pH values [28].

Approximately 2,500 million cubic meters of mineral oil used annually in the Occupied Palestinian Territory is released without any collection or adequate collection systems. Small steel mills in the occupied Palestinian territories use a range of hazardous substances such as heavy metals, phenols (and their salts), dioxins, furans, cyanides and many hazardous halogenated hydrocarbons [29].

2.4 Adsorption

Is the sticking of atoms, ions or molecules from a gas, liquid or dissolved solid to a surface **[30]**. This process creates a film of the adsorbate on the surface of the adsorbent. Adsorption is a surface-based process.

Adsorption is found in many natural, chemical, biological and physical phenomena and is widely used in industrial applications such as heterogeneous catalysts, activated charcoal, capture and increased storage capacity of carbonate derived from carbide and water purification. Adsorption and ion exchange and chromatography are absorption processes in which selective adsorbents are transferred from the liquid phase to the surface of insoluble, rigid molecules suspended in a pot or packed in a column. Pharmaceutical industry applications **[31]**.

2.4.1 Adsorption phenomenon

Adsorption is a surface phenomenon with common mechanism for organic and inorganic pollutants removal. When a solution containing absorbable solute comes into contact with a solid with a highly porous surface structure, liquid–solid intermolecular forces of attraction cause some of the solute molecules from the solution to be concentrated or deposited at the solid surface. The solute retained on the solid surface in adsorption processes is called adsorbate, whereas, the solid on which it is retained is called as an adsorbent. This surface accumulation of adsorbate on adsorbent is called adsorption. This creation of an adsorbed phase having a composition different from that of the bulk fluid phase forms the basis of separation by adsorption technology **[32]**.

As I mentioned earlier, adsorption is another mass transfer process in which the material is transferred from the liquid phase to the surface of the solid and becomes bound by physical and / or chemical reactions. Large area lead to high adsorption capacity and surface interaction **[33]**.

Adsorption is a consequence of surface energy. In a bulk material, all the bonding requirements (be they ionic, covalent or metallic) of the constituent atoms of the material are filled by other atoms in the material.

However, atoms on the surface of the adsorbent are not wholly surrounded by other adsorbent atoms and therefore can attract adsorbates. The exact nature of the bonding depends on the details of the species involved, but the adsorption process is generally classified as physisorption (characteristic of weak van der Waals forces) or chemisorption (characteristic of covalent bonding). It may also occur due to electrostatic attraction **[34]**.

2.4.2 Adsorption Isotherms Models

Equilibrium study on adsorption provides information on the capacity of the adsorbent. An adsorption isotherm is characterized by certain constant values, which express the surface properties and affinity of the adsorbent and can also be used to compare the adsorptive capacities of the adsorbent for different pollutants. Equilibrium data can be analyzed using commonly known adsorption systems. Several mathematical models can be used to describe experimental data of adsorption isotherms. The Freundlich, Langmuir and Temkin models are employed to analysis adsorption occurred in the experiment. [35] Data of adsorption isotherms. The Freundlich, Langmuir and Temkin models are employed to analysis adsorption occurred in the experiment.

There is a wide range of equilibrium isotherm models. Langmuir, Freundlich, Brunner-Imit-Tiller, Redlich-Peterson, Thoth, Kobli-Corrigan, Sibs, Khan, Hill, Flory-Hughes and Radk-Brausnitz-Esoterm were formulated in three basic approaches [36] . Motorization is the first approach to be transmitted. Here, the absorption balance is defined as a state of dynamic equilibrium, with both absorption and adsorption rates equal. While thermodynamics, being the basis of the second approach, can provide a framework of derivation of many forms of isotherm absorption models, and potential theory, as the third approach, usually conveys the main idea in the generation of characteristic curve. However, an interesting trend in the isotherm modeling is the derivation in more than one approach, thus directing to the difference in the physical interpretation of the model parameters [37].

2.4.2.1 Langmuir Adsorption Isotherm

The Langmuir adsorption model is the most common model used to quantify the amount of adsorbate on an adsorbent as a function of partial pressure or concentration at a given temperature. This describes quantitatively the formation of a single layer adsorbate on the outer surface of the adsorbent, and after that no further adsorption takes place. Thereby, the Langmuir represents the equilibrium distribution of Cyanide between the solid and liquid phases. The Langmuir isotherm is valid for singlelayer adsorption onto a surface containing a finite number of identical sites. The model assumes uniform energies of adsorption onto the surface and no transmigration of adsorbate in the plane of the surface.

The Langmuir equation relates the coverage of molecules on a solid surface to the concentration of a medium above the solid surface at a fixed temperature. This equation can be written as:

$$\frac{1}{q_e} = \frac{1}{q_0} + \frac{1}{q_e K_L C_e} \qquad (2.1)$$

Where:

Ce = the equilibrium concentration of adsorbate (mg/L)

qo = maximum monolayer coverage capacity (mg/g)

KL = Langmuir isotherm constant (L/mg).

qe is the amount of adsorbate per unit mass of adsorbent (mg/g) [38], and it can be calculated using the following relation:

$$\mathbf{q_e = (C_o - C_e) \frac{V}{m}} \qquad (2.2)$$

Where:

Co is the initial concentration of the adsorbate (mg/L).

V is the volume of the solution (L).

m is the mass of the adsorbent (g).

(Co – Ce) represents the adsorbed amount (ppm). A graph of (Ce/qe) values versus Ce is used to find the Langmuir parameters. That are, (1/KLQo) as y-intercept and (1/qo) as slope [39].

The essential features of the Langmuir isotherm can be expressed in terms of a dimensionless constant separation factor RLwhich is given by the following equation [40] :

$$\mathbf{R_L} = \frac{\mathbf{1}}{\mathbf{1+ K_{LC_0}}} \tag{2.3}$$

Where:

C0 = initial concentration.

KL = the constant related to the energy of adsorption (Langmuir Constant). RL value indicates the isotherm shape to be unfavorable if (RL >1) Linear if (RL = 1), favorable if (0 <RL <1), or irreversible if (RL = 0) [41].

2.4.2.2 Freundlich model Isotherm

The Freundlich isotherm model applies to adsorption on heterogeneous surfaces with interaction between the adsorbed molecules, and is not restricted to the formation of a monolayer. This model assumes that as the adsorbate concentration increases, the concentration of adsorbate on the adsorbent surface also increases and, correspondingly, the sorption energy exponentially decreases on completion of the sorption centres of the adsorbent. The well-known expression for the Freundlich model is given as [39,42].

$$\ln \boldsymbol{q_e} = \ln \boldsymbol{K_F} + \frac{\mathbf{1}}{\boldsymbol{n}} \ln \boldsymbol{C_e} \tag{2.4}$$

Where:

KF is the Freundlich constant which indicates the adsorption capacity of the sorbent (mg/g).

n is the heterogeneity coefficient that gives an indication of the Favorable way

of the adsorption process (g/L)m if the value of 1/n is less than one then the adsorption is normal ,and if n is between one and 10, the sorption process is favorable .

A plot of Lnqe values versus LnCe is used to find Freundlich parameters. That are, LnKF as y-intercept and (1/n) as a slope.

If the temperature is raised, both the K and N parameters change to reflect the experimental observation that the adsorbent quantity rises more slowly and the higher pressures required to saturate the surface [43].

2.4.3Adsorption Thermodynamics

The basis for thermodynamic calculations is the adsorption isotherm, which gives the amount of gas adsorbed in the nanopores as a function of the external pressure. Adsorption isotherms are measured experimentally or calculated from theory using molecular simulations. Potential functions are used to construct a detailed molecular model for atom–atom interactions and a distribution of point charges is used to reproduce the polarity of the solid material and the adsorbing molecules

Adsorption thermodynamics were determined using the thermodynamic equilibrium coefficients obtained at different temperatures and concentrations in order to verify possible adsorption mechanisms. The adsorption characteristics of a material can be expressed in terms of thermodynamic parameters such as ΔG (Gibbs free energy change), The general equation which connects between the adsorption parameters can be written as [44-46]:

$$\Delta \mathbf{G} = \Delta \mathbf{H} - \mathbf{T}\,\Delta \mathbf{S} \tag{2.5}$$

Where:

T is the absolute temperature (K).

The change in Gibbs free energy can be also calculated by the following equation:

$$\Delta \mathbf{G} = -\mathbf{R}\,\mathbf{T}\,\ln \boldsymbol{K_d} \tag{2.6}$$

Where:

R is the universal gas constant that equals 8.314 J.mol-1.K-1.

Kd is the thermodynamic equilibrium constant that equals (qe/Ce) with a unit of mol or (L/g).

The combination of the previous two equations will give the following equation:

$$\ln \boldsymbol{K_d} = \frac{\boldsymbol{\Delta S}}{\boldsymbol{R}} - \frac{\boldsymbol{\Delta H}}{\boldsymbol{RT}} \tag{2.7}$$

The plot of LnKd versus (1/T) will give a straight line with (-ΔH/R) as slope and (ΔS/R) as y-intercept. The resulting graph is known as Van’t Hoff plot.

2.4.3.1 Adsorption kinetics

Kinetic study provides important information about the mechanism of cyanide adsorption onto Graphene- CoFe2O4 Magnetic.

Fitting the experimental data into different kinetic models enables to study the adsorption rate, model the process and predict information about adsorbent/adsorbate interaction. In this study. Pseudo first-order and second- order kinetic models were tested in this study where experimental data obtained for the different contact times were used.

The linear form of pseudo-first-order kinetic model is generally expressed by the following equation[47,48]:

$$\ln(q_e - q_t) = \ln q_e - K_1 t \tag{2.8}$$

Where:

qe and qt are the amounts of adsorbate adsorbed per unit mass of adsorbent at equilibrium, and at time t respectively (mg/g).

k1 is the pseudo first-order rate constant for adsorption (min-1).

A plot of Ln (qe−qt) versus t should give a linear relationship that allows the computation of a first-order rate constants.

The pseudo second order kinetics can be expressed in a linear form as integrated second order rate law [47,49]:

$$\frac{t}{q_t} = \frac{1}{K_{2q_e^2}} = \frac{t}{q_e} \qquad (2.9)$$

Where;

k_2 is the pseudo second-order rate constant for adsorption ($g.mg^{-1}.min^{1}$).

The plot of t/qt versus t will give a straight line for the pseudo second order adsorption with (1/ K2 qe2)as y-intercept and (1 /qe) as the slope of the graph [50].

The second-order pseudo-system relies on absorption and absorption and involves chemisorption as well as physiotherapy. Chemisorption may be a step reduction rate where valence forces are involved by exchanging electrons or exchanging adsorbents and perseverance.

The Intra-Particle Diffusion Kinetic Model is established on the theory suggested by Weber and Morris. The final equation of this adsorption kinetic model can be written as:

$$\mathbf{q_t = K_{id}\, t^{1/2} + Z} \qquad (2.10)$$

Where;

Kid is the Intra-Particle diffusion rate constant (mg/g.min1/2).

Z is a constant that gives an information about the thickness of the boundary layer (mg/g) [51].

A plot of qt versus t1/2 will give a linear relationship for intra-particle diffusion kinetic model with constant Z as a y-intercept and Kid as a slope.

2.4.3.2Type s of adsorbents

Major types of adsorbents in use are: activated alumina, silica gel, activated carbon, and polymeric adsorbents .There are several types of adsorbents in natural adsorbents and synthetic additives. Natural adsorbents contain zeolite, clay, clay minerals, coal, and ores. These materials are natural, since these materials are considered inexpensive in most cases, abundant in supply and have great potential to modify and ultimately enhance their absorption capacities. Synthetic sorbents are adsorbents prepared from agricultural products and waste, household waste, industrial waste, sludge sludge and polymer capacitors. All adsorbents have their own properties such as porosity, pore structure and the nature of adsorption surfaces. Many used wastes include fruit waste, coconut husk, scrap tires, bark, and other materials rich in tannin, sawdust, rice husks, petroleum wastes, fertilizer wastes, fly ash, sugar industry, slag waste, rock kilns, shitosan and seaweed, seaweed, algae, peat moss, clays, red mud, zeolites, sediment and soil, ore minerals etc. [32].

2.4.3.3 Adsorption as an effective method for removing cyanide from wastewater

Adsorption is an important process for cyanide removal as it is simple to operate and no hazardous chemicals are required in this process. The most common adsorbent used for cyanide removal is plain or modified activated carbon, which has a quite low cyanide adsorption capacity and high regeneration cost [52]. To make the adsorption process attractive and achievable, novel low-cost adsorbents with high adsorption capacities are required. Various agro based materials have been widely reported for their ability to remove different contaminants from water and wastewater [53].

Within the several processes to remove such contaminants from water. These can be divided into physical, chemical, and biological methods. Among the various methods adsorption is a top remediation technology in terms of low costs adsorbents, flexibility and simplicity of design, easy operation and high efficiency [54,55]. Cyanide adsorptive removal studies are reported using several different materials, such as zeolite combined with polyaniline [56] and layered double hydroxides [57].

Due to the wide diversity of nanomaterials for absorption, Graphene (G), emerging as new carbon materials with a single two-dimensional atom thickness, attracted wide interest from the scientific community due to its mechanical, electrical, thermal and optical properties, Surface is very high [58]. Although graphene and Graphene Oxide (GO) are good condensates for many contaminants, effective removal of water after treatment is still a challenge [59]. To overcome this issue, the innovative technology that has gained great interest is the use of magnetic materials for easy separation

Because cyanide has very little cyanide, simple methods are not very effective in treating cyanide water. They are usually treated either by physical or chemical processes. However, these processes are very expensive and can not be used effectively to treat a wide range. The process of adsorption is one of the effective ways to remove cyanide from wastewater. The adsorption process has an advantage over other roads due to a clean process free of sludge.

Adsorption has been found to be superior to other techniques for water reuse in terms of initial cost, flexibility and simplicity of design and ease of operation [60].

Adsorption is important as it can economically meet the highest standards of effluents today. It may be considered as an essential process in the physico-chemical treatment of municipal wastewater. Adsorption is an integral part of a wide range of physical, biological, and chemical processes and processes in the environmental field. This process has proved to be widely effective for the removal of dissolved organic matter from wastewater, but it should not be viewed as Catholic waste treatment and should not be applied in an experimental

Graphene is an allotrope of carbon consisting of a single layer of carbon atoms arranged in a hexagonal lattice. It is the basic structural element of many other allotropes of carbon, such as graphite, charcoal, carbon nanotube and fullerenes.

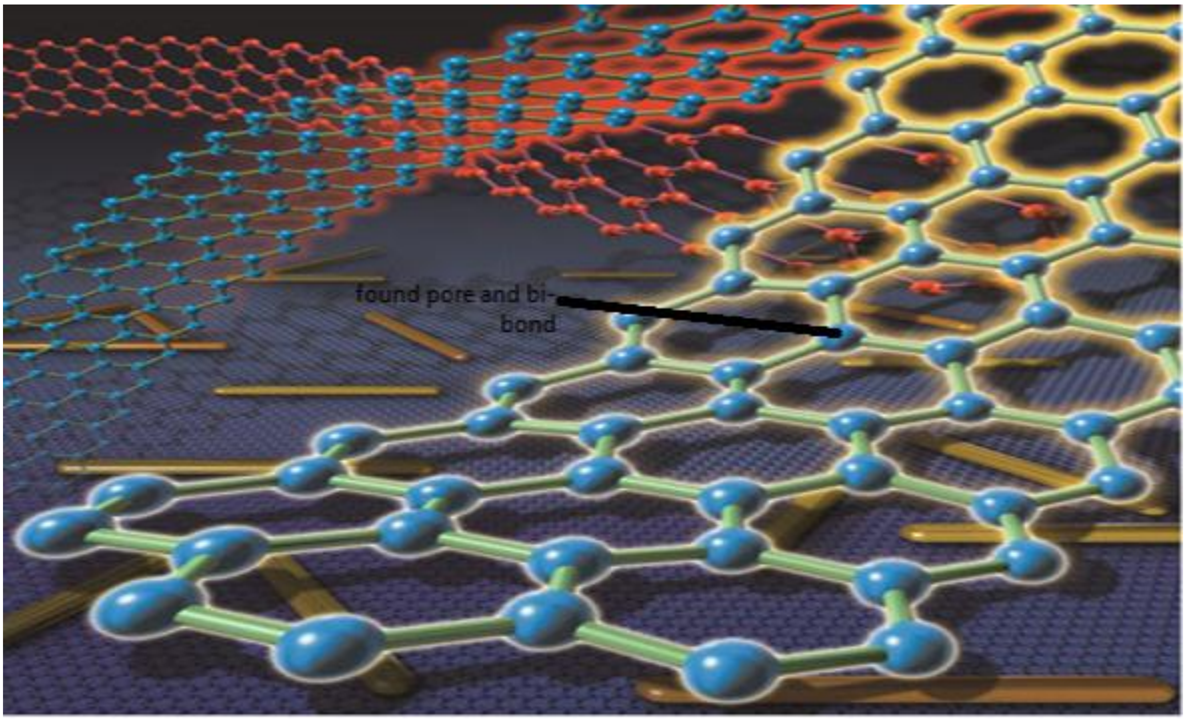

Fig: 2.2 shape of graphene

Since graphene has p-p bond, it has a large number of conductive electrons and also has a high surface area, which makes it good for adsorption.

Chapter Three
Experimental Work

3.1Chemicals and Materials

All solvents and chemicals were of analytical scale and used without additional purification. Cobalt Chloride ($CoCl_2$ $6H_2O$ purity ≥ 98.5). Ferric Chloride ($FeCl_3$ $6H_2O$ purity ≥ 99%). Graphite, Sodium Acetate Anhydrous (NaAc, >99% Sigma Aldrich) Distilled water was used to prepare stock solution and used in all process of aqueous solutions, suspensions and washing. HNO_3 (0.1M) and KOH (0.1M) for pH adjustment were used, Hydrochloric acid (HCl, 36%), Sulfuric acid (H_2SO_4, 95–98%), Potassium Persulfate ($K_2S_2O_8$, 99–100%), Isonicotinic Acid (4-Pyridinecarboxylic Acid Sigma Aldrich), Barbituric Acid(Sigma Aldrich), one percent (weight/volume) Chloramine-T solution(Sigma Aldrich).

The required materials and apparatus are: glassware, scale, UV-visible spectrophotometer (model: UV-1601, SHIMADZU), pH meter (model: 3510, JENWAY),Fourier Transform Infrared (FT-IR) is used for recording and measuring spectra[Thermal Scientific,ID3 ATR],Centrifuge (model:1020 DE, Centurion Scientific), Thermal Gravimetric Analysis (TGA) of Q60 V20.10 Build 36 tool with average of heating 50◦C/min and in N2 the atmosphere of gaseous Differential Scanning Calorimeter (DSC) Q200, TA Instruments, desiccator.

3.2 Synthesis of $CoFe_2O_4$ Nanoparticles

The synthesis was conducted at university of Castilla la Mancha in Spain by Prof. Dr. Shehdeh Jodeh and Carlos Adelantado as follows, 2.6 g out of Iron(III) Chloride Hexahydrate and 0.854 g out of Cobalt(II) Chloride Hexahydrate were exactly melted in 100 mL water of deionized so that the percentage of Mn:Fe in the solution be 1:2. The fixed solution was stirred and heated to 80 °C. For than, 8 M sodium hydroxide was heated to similar temperature and was added slowly (frequent stirring) in order to increase the pH of the solution to 11.5. All of the above material in beaker are continued for 5 minutes then last the temperature was reduced to 25 Celsius. The precipitates of blackish were separated with using magnetically and cleaned with extra water to eliminate the unreacted content then after clean with acetone. Then, the precipitates are dried at steady temperature of the room a one day.

3.3 Synthesis of $GO-CoFe_2O_4$ Nanohybrids

The synthesis was conducted at university of Castilla la Mancha in Spain by Prof. Dr. Shehdeh Jodeh and Carlos Adelantado as follows, It was added (0.5 g) from Graphene Oxide to 400 mL of water and distributed by ultrasonication last for 5 minutes. At the same time, 2.6 g out of Iron(III) Chloride Hexahydrate and 0.854 g out of Cobalt(II) Chloride Hexahydrate were added to the solution of colloidal graphene oxide and stirred for 30 minutes. The solution temperature was increase to 80 °C with continuous stirring conditions. Then, the solution of pH was increased to 11.5 by adding 8 M sodium hydroxide (heated to the same temperature). The interaction was continued for the same duration for five minutes and then cooled to the temperature of the room which was 25C. The particles of nanohybrid were separated with a magnetic and cleaned with extra acetone and water. The precipitates were dried at room temperature for a day.

3.4 Characterization of GO−$CoFe_2O_4$ Nanohybrids

The characterization was conducted at university of Malaga in Spain by prof. Dr. Manuel Algarra, the Fourier Transform Infrared spectrum of the graphene oxide , the merits peaks of graphene oxide and nanoparticle. These finding reveal that the nanohybrids and the typical Scanning Electron Micrograph (SEM) successfully prepared. As a result, the nanoparticles on graphene was found to be in harmony various samples.

3.5 Preparation of cyanide solutions

About 0.5 g of Potassium Cyanide is taken in a 500 mL volumetric flask to prepare; 5, 10, 15, 20, 25, 30, 40 and 50 mg/L.

3.5.1 Preparation of isonicotinic acid-barbituric acid

In brief, the inside tube of dried reaction, put 10.0ml of sample solution around value (pH 5-8) consisting of 25mg Cyanide, without thiocyanate and Sulfide ions. Add 3.0 ml of $K(H_2PO_4)$ solution (1M) and 0.2ml of one percent (w/v) Chloramine-T solution, close the tube then shake it gently. Add 5.0 ml of isonicotinic acid-barbituric acid reagent after 1-2 min, close the tube again, mix it, and keep the mixture at 25°C for 15 min [61].

3.6 Calibration Curve

A spectrophotometric method for the determination of Cyanide in water with an isonicotinic acid-barbituric acid reagent having no offensive odor of pyridine is described. Cyanide reacts with chloramine-T, and then the reagent is added to form a soluble violet-blue product, which is measured at 600 nm .

The concentration of Cyanide is analyzed by UV-visible Spectrophotometer (UV-1601 SHIMADZU). A standard Cyanide solution of 1000 mg/L is prepared and absorbance is determined at various wavelengths to obtain a representative plot of absorbance versus wavelength (Figure 3.1). The wavelength related to the maximum absorbance which determined from this plot is 600 nm.

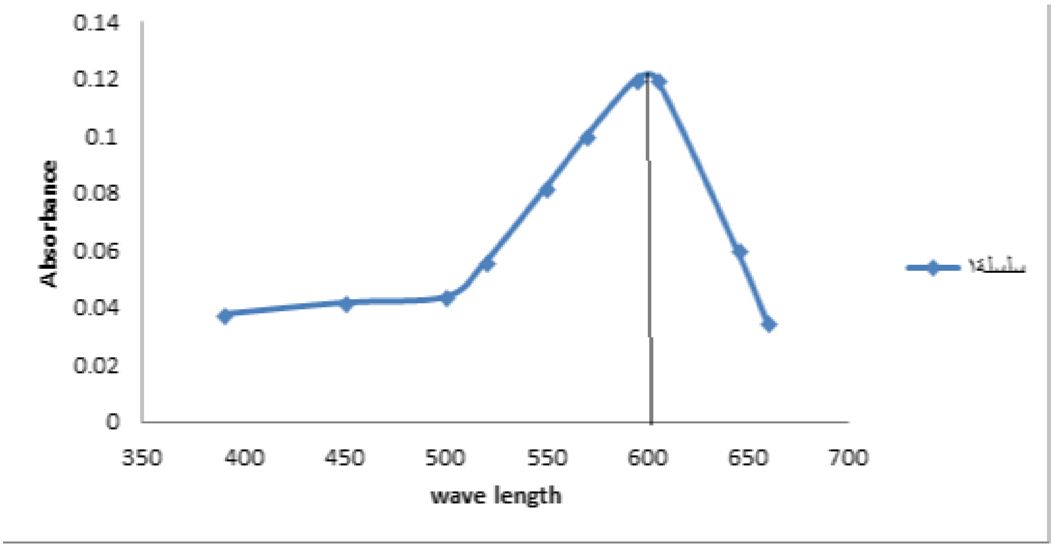

Figure 3.1: A representative plot of absorbance versus wavelength for a Cyanide complex.

With high focus of cyanide, Beer-Lambert relation deviates from linearity. As a result, it gives a non-linear relationship, as revealed in Figure 3.2, so the researcher is worked limited at concentration up to 25 mg/L. At higher concentrations, the single pieces of analyte will not behave independently of each other. The result of the interaction between particles for the analyte changes value of ε. Also the absorption capacity (a) and molar absorptivity (ε) depend on the sample refractive index. Since the refractive index varies with the concentration of the analyte, the values of a and ε change. At enough low concentrations of analyte, the refractive index remains constant, and the calibration curve show in fig3.3. Few large ions or molecules deviate from Beer-Lambert law even at low concentrationns.

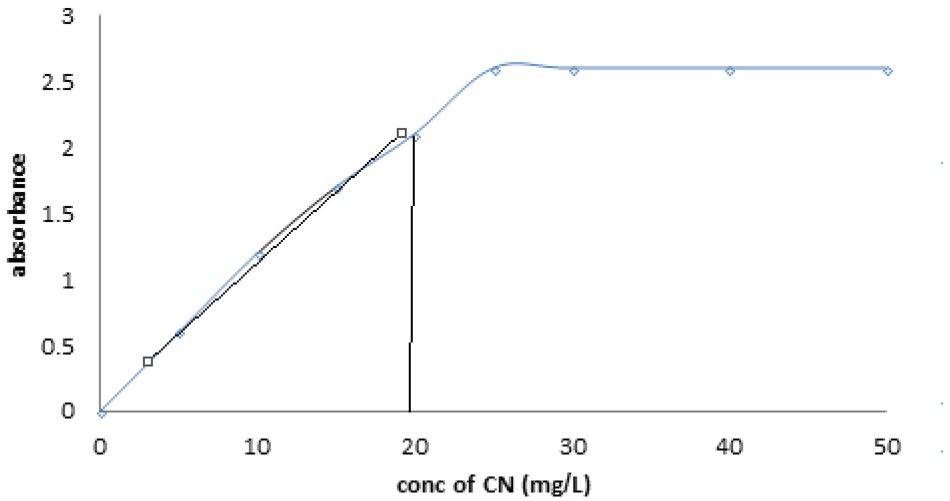

Figure 3.2: A representative plot of the absorbance versus concentration of Cyanide solution.

Linear calibration curve between the absorbance and the concentration was obtained with Cyanide concentrations in the range 5-20 mg/L ($R^2 = 0.9933$) as shown in Figure 3.3.

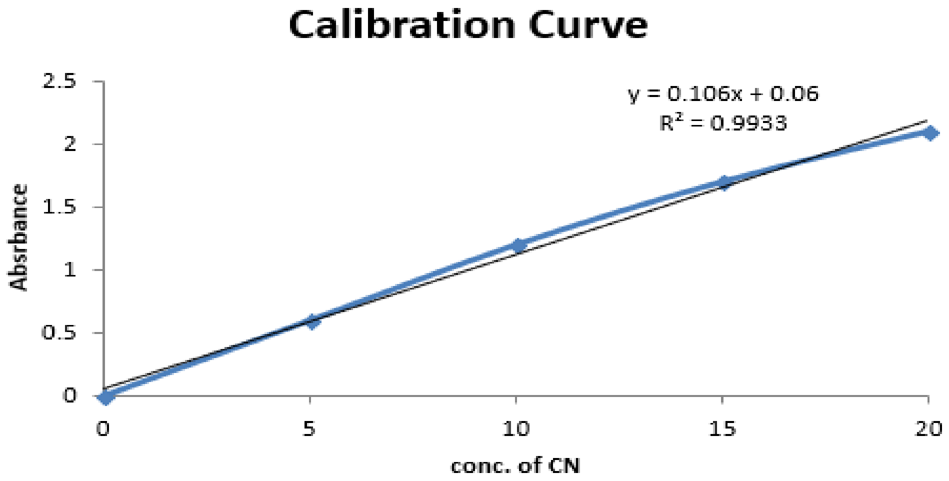

Figure 3.3: Linear calibration curve of absorbance vs. concentration for CN concentrations in the range 5-20 mg/L.

3.7 Adsorption Experiments

The maximum absorbance (λmax= 600 nm) as determined from the plot was used for measuring the absorbance of residual concentration of cyanide. The pH of solutions is controlled by using nearly intensity of (0.1M) HNO_3 and (0.1M) KOH. By conducting batch mode experimental studies the efficiency of the adsorbent was evaluated. The adsorption behavior of the new surface with cyanide was studied. The effect of pH, temperature, dose of adsorbent, concentration of cyanide solution and the contact time on the adsorption of Cyanide was studied. The adsorption capacity of is examined by using kinetics and pH effects. Equilibrium isotherm research that conducted by varying the following parameters:

initial concentration of Cyanide solution, temperature, and adsorbent have great effect on Cyanide adsorption from the solution. At the end of experience, the adsorbent is eliminated by centrifuging at 600 rpm. The supernatant is analyzed by UV-visible spectrophotometer for the residual concentration of Cyanide, at 600 nm wavelength.

The proportion of cyanide removal (% Removal) is recognized as percentage of disparity of cyanide concentricity pre and post adsorption to the beginning focusing for Cyanide in aqueous solution and was calculated by the following equation [21,42]:

$$\mathbf{Removal\ efficiency}(\%) = \left[\frac{(\mathbf{C_o} - \mathbf{C_f})}{\mathbf{C_o}}\right] \times \mathbf{100} \qquad (3.1)$$

Where, Co is the Initial Cyanide concentration (mg/L) in the sample and Ce is The final Cyanide concentration in the sample solution after treatment.

3.7.1 Experiment (1) • The temperature effect

For studying the temperature effect on adsorption, 0.10 g adsorbent samples were added to 50 mL of Cyanide solutions with concentration 20 mg/L at pH 7. Each solution stirred using Water bowl (Daihan Labtech) at range 15-45 Celsius for 25 min. At the end of each time interval, the adsorbent is separated by centrifuging at 600 rpm and supernatant was tested by UV-visible spectrophotometer (UV-1601, SHIMADZU) for the residual concentration of Cyanide, at 600 nm wavelength.

3.7.2 Experiment (2). The pH effects

The influence of initial acidity or alkalinity of a solution on adsorption is examined in the pH range 3-12. The NaOH and HCl are used to modify the degree of acidity, so the result are 0.05 g adsorbent samples are added to 20 mL of CN solutions with concentration 20 mg/l. The combination is put inside the bowl at fixed temperature (25°C) for 25 min. At the end of each time interval, the adsorbent is separated by centrifuging at 600 rpm and supernatant was analyzed by UV-visible spectrophotometer for the residual concentration of CN, at 600 nm wavelength.

3.7.3 Experiment (3) • Effect of initial concentration of cyanide

To explore the best conditioning focus, 0.1 g of adsorbent is add up to a number of tube consist of 20 mL of different focused of cyanide solution (5-50 mg/L), under optimized temperature (15oC) and pH 3 for 25 min. The absorbance of the solution above the solid residue was measured by UV-spectrophotometer

3.7.4 Experiment (5) • Optimization of contact time

To examine the adsorption kinetics, different concentrations (5-50 mg/L) are taken by using adjusting 0.2504 g adsorbent dosage, after that it by shaker, mixtures are agitated at 600 rpm and 15°C . The supernatant is carefully removed by a thin plastic dropper and absorbance was measured by UV-visible at 600

3.7.5 Experiment (4). The influence of adsorbent dose

The influence of adsorbent dosage on cyanide system adsorption is studied. 0.015, 0.05, 0.10, 0.15 and 0.20 g of a substance that adsorbs cyanide are add up to five tube consist of 20 mL of 15mg/L cyanide solution at pH 3 to examine the best adsorbent dose, The combination are put in moving water bowl at fixed temperature (15°C) for 25 min. The absorbance of the solution above the solid residue was measured by UV-visible for the residual concentration of CN.

3.8 Thermodynamics and Kinetics of Adsorption

The removal of cyanide has been studied using adsorption technology using prepared absorbent materials graphene oxide ($M-CoFe_2O_4$ / GO) . The method is organized under the optimal state of contact time, adsorption dose, initial concentration of cyanide, temperature and pH. Before and after adsorption, the cyanide concentration is measured by using the UV scale. Langmuir, Freundleich Isotherm adsorption equations were studied. The corresponding parameter values were determined. Thermal parameters such as free energy (□G°), anthalby (□H°) and entropy (□S°) were calculated from the systems using the Van Hoof plot. The values of % removal and coding of dye systems were worked out at various temperatures ranging from 15 - 45 ^{O}C.

Adsorbent (0.1 g) was added to 50 mL of (5,15,25 mg/L) of CN solution at pH 3. The combination is put in moving water bowl at fixed temperature (15°C). Adsorption rate is monitored by studying the contact time up to 5 h and compared to theoretical models. The first pseudo and the second pseudo order kinetic models were tested in this study where the experimental data obtained for various contact time were used. The first pseudo and the second pseudo order kinetic model parameters (K, Qe and R2) for CN adsorption M−CoFe2O4 /GO.

Chapter Four

Results and Discussion

4.1 Modified *Magnetic- $CoFe_2O_4$ Graphene oxide Nanohybrids* (MGONH) Characterization.

Some properties of the compound have been achieved through several techniques, including an X-ray Analysis. Spectrum FTIR, TGA and others.

4.1.1 SEM Analysis of the Modified graphene oxide

Scanning Electronic Microscope (SEM) analysis was performed. Images were collected at 10 micrometer are shown in (Figure 4.1) and were performed to give information on the physical appearance of the modified MGONH surface.

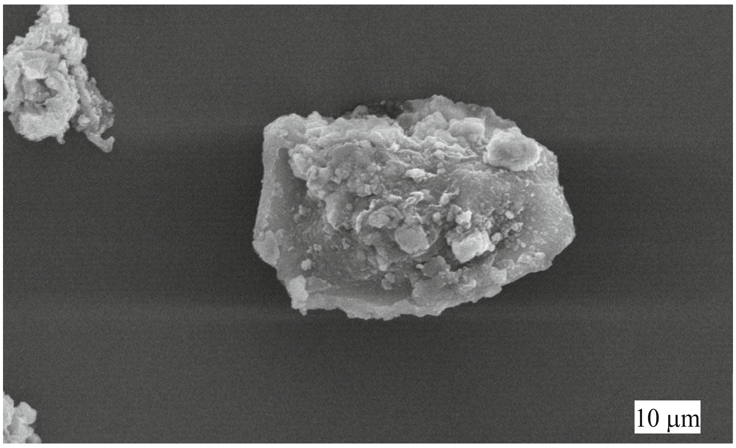

Figure 4.1: SEM micrographs of the modified graphene oxide [62].

SEM images of surface MGONH modified coarse exhibit and nature burede, showing that the material shows good properties for use as absorbent materials.

Through the image in Figure 4.1 of the magnetic GO-CoFe2O4 compound, this magnetic surface of the body is relatively smooth, the particle size is homogeneous, and the diameter is about 10 µm.

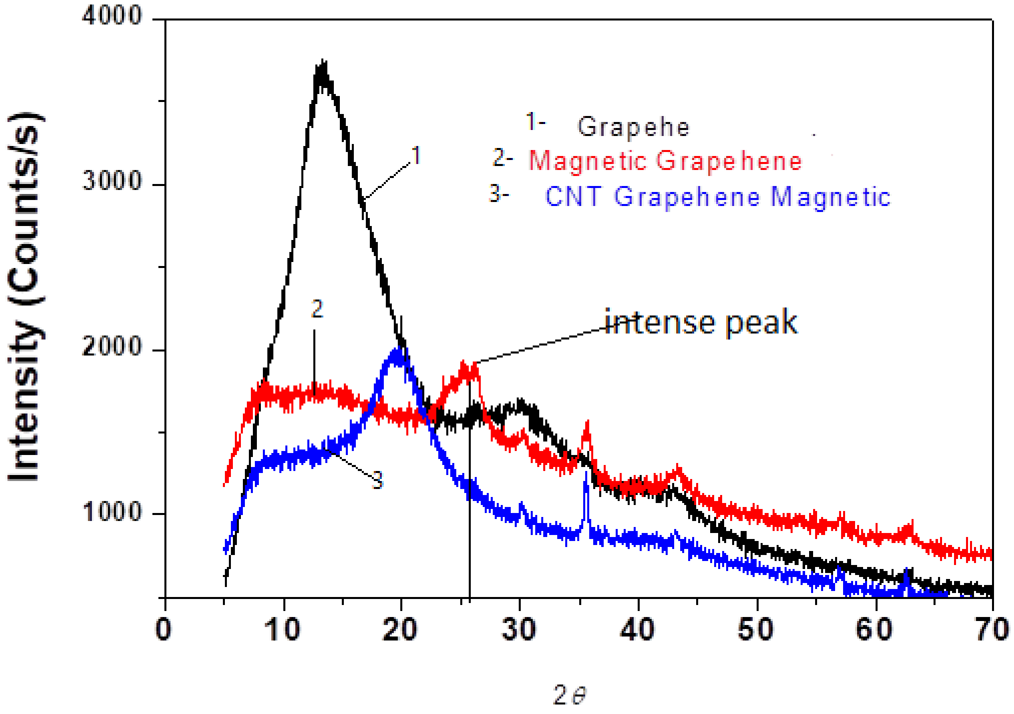

Figure 4.2: X-ray diffraction spectra of number (2) line for Magnetic Graphene.

This curve represents the relationship between the degree and density, shown on the line number (2) of the Figure 4.2 number of crystal planes , The most intense peak is observed at degree value of 25.43.

4.1.2 FT-IR And ATR Characterization

This technique uses the FT-IR spectrum to determine the structure. The FT-IR spectra can help provide information on the redistribution of cations between eight surfaces and tetrahedral locations of the inverse spinel structure in GO.

In Figure 4.3, shows the FTIR spectra for the GO. The FTIR spectrum showed a wide characteristic band around 3434 cm-1 can be assigned to hydrogen bonded O–H stretching vibration arising from surface hydroxyl groups on nanoparticles. Another characteristic band, associated with the presence of structural water, is visible at 1630 cm-1. The bands at 2921 and 2849 cm-1 were assigned to stretching of C–H groups and the bands at 1387–1084 cm-1 to C–O stretching surface, A long peak at 1600 cm-1 with another in 1700 (C=O), 2362 signal is due to caboxylic acid, and then in 1627(C=C) aromatic ring.

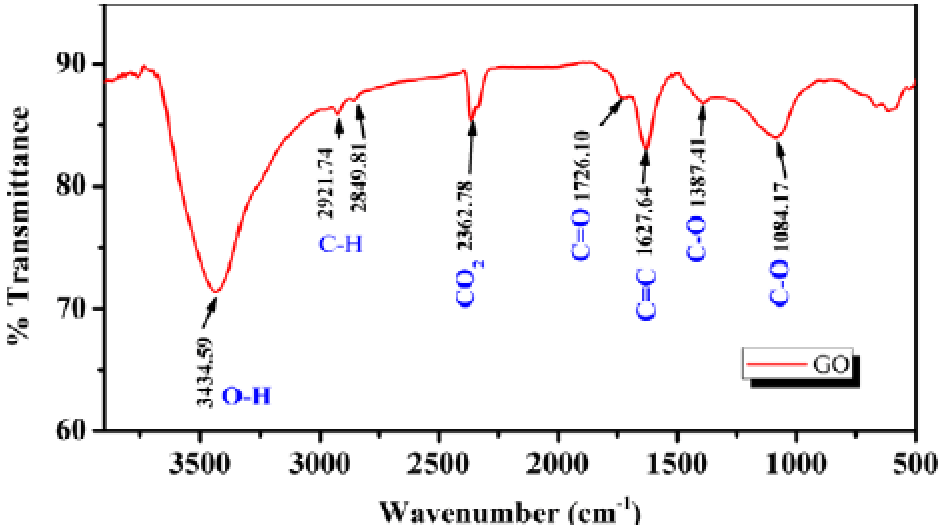

Figure 4.3: FTIR spectra to the graphene oxide (COFe2O4) [55].

4.1.2.1 ATR Characterization:

Attenuated total reflection (ATR) is a sampling technique used in conjunction with infrared spectroscopy which enables samples to be examined directly in the solid or liquid state without further preparation.

ATR uses a property of total internal reflection resulting in an evanescent wave. A beam of infrared light is passed through the ATR crystal in such a way that it reflects at least once off the internal surface in contact with the sample. This reflection forms the evanescent wave which extends into the sample. The penetration depth into the sample is typically between 0.5 and 2 micrometres, with the exact value being determined by the wavelength of light, the angle of incidence and the indices of refraction for the ATR crystal and the medium being probed [63]. The Figure 4.4 shows that there is no high spectral features and this indicates that the crystal is clean.

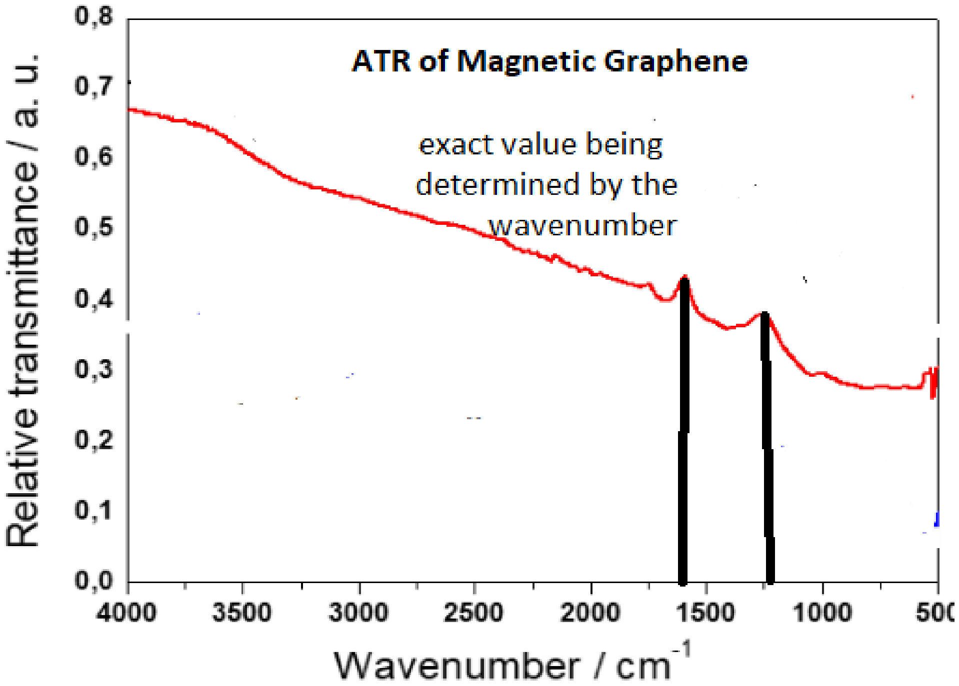

Figure 4.4: ATR for the Magnetic Graphene.

\

4.1.3 TGA Analysis

Thermo Gravimetric Analysis (TGA) is the measurement of the weight loss or gain as a function of temperature or time. It can be used to calculate the components in a polymer or material.

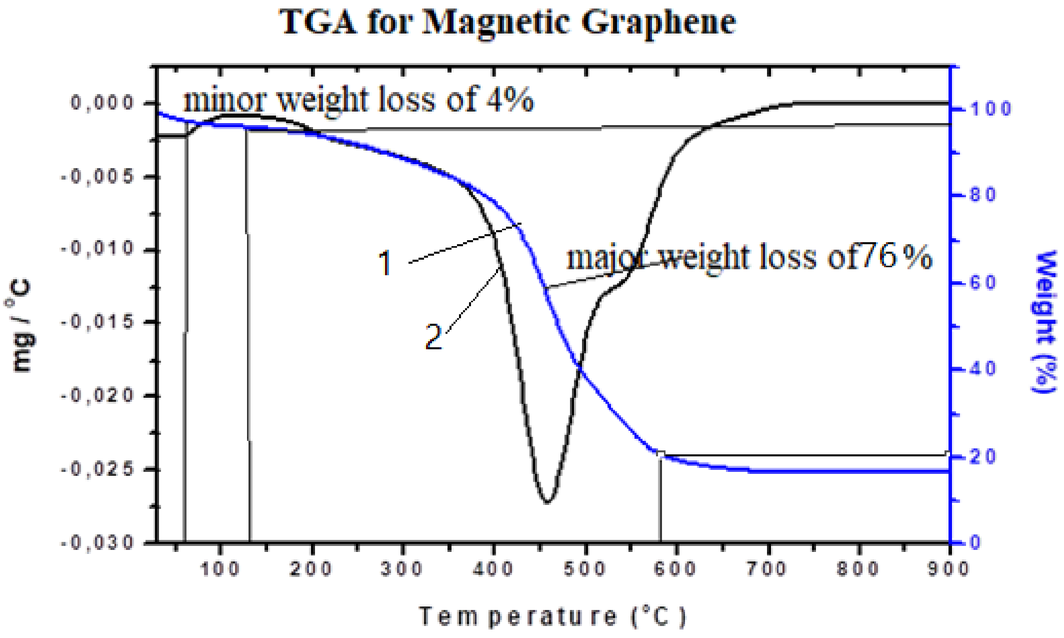

Figure 4.5: TGA curve of a Magnetic Graphene with TEG.

In Fig. 4.5, The TG thermogram in the line number (1) showed a minor weight loss of 4% between 55 and 130 °C due to the loss of physically adsorbed water. The major weight loss of 76% in the temperature range of 130–570 °C was due to the burning off of adsorbed TEG in the sample. The weight was stabilized above 570 °C indicating all decomposition processes being completed. The presence of adsorbed cyanide entities on the surface of the CoFe2O4 was also proven by TG measurements.

4.1.3.1 Thermal Stability

Differential Scanning Calorimetry (DSC) can be Measuring the flow of heat against the temperature of graphene oxide. The flow temperature of the heat flow can be used to determine the melting, crystallization, and transition temperature of the glass material in the form of the line number (1) peak showing in (Fig.4.6) the point at which the different crystalline components of the graphene oxide melted at a temperature of approximately 445 Celsius.

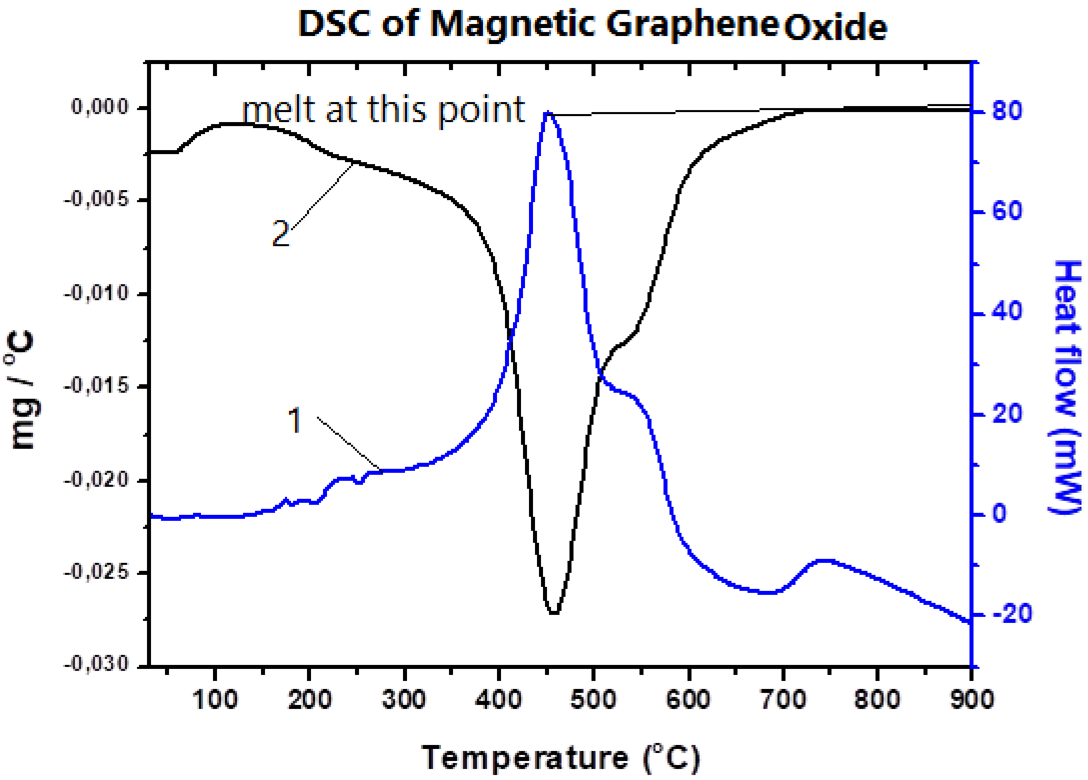

Figure 4.6: DSC measurement of heat flow versus temperature for graphene oxide.

4.1.4 Analysis CoFe2O4–GO substrates by TEM and Variable Scanning Magnetometry (VSM).

Delegate Electron Microscopy Transfer (TEM), Images of nanoparticles graphene in Figs. 4.7 .The dark spots shown in Figure (red arrow) in plate are cobalt ions divided between graphene sheets. High-resolution images TEM Flat planes appear graphene.

As seen from the images, the Graphene Oxide (GO) nanoparticles diameter were varied from 50 to 500 nm and the $CoFe_2O_4$ nanoparticles were the aggregation of a great number of smaller nanoparticles with an average size of 10–15 nm and exhibits porous structure. graphene oxide and $CoFe_2O_4$ spheres were decorated on flake. Hence, it could be confirmed from the below analysis that the Cyanide coated $CoFe_2O_4$ nanoparticles were homogeneously decorated on graphene oxide.

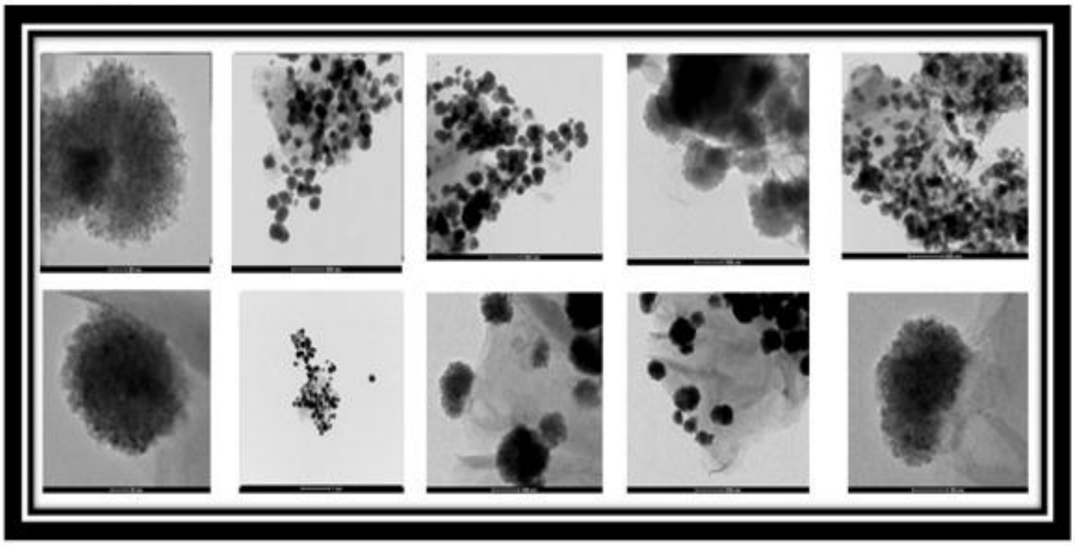

Figure 4.7: TEM Analysis of the Modified Magnetic $CoFe_2O_4$ /GO.

The TEM image of the $CoFe_2O_4$ magnetic compound is shown in Figure 4.7. This apparent dispersion in the picture was not suitable for magnetism. This may be because the particle size is small, and the magnetic field has a strong impact on the particles. Another reason is the presence of a conglomerate of nanoparticles in the solution. However, we note from the picture that the microscopy is regular sizes and has spherical and comparatively smooth surface. The microscopic diameter was about 1 μm.

4.2 Investigation of adsorption parameters

4.2.1 Effect of pH on Cyanide adsorption

The pH of a solution is an important factor that influences the removal efficiency of CN on Magnetic $CoFe_2O_4$ Graphene Oxide Nanohybride (MGONH) under different initial pH are shown in Fig.4.8, It can be seen that the CN adsorption on MGONH is effective and pH has no obvious influence on CN removal in the whole experimental pH (Fig. 4.8). In detail, CN adsorption gradually increases with the increasing of pH and the removal efficiency is over 91% at pH about 3. The results show that as the pH increases up to 3, the adsorption of Cyanide will be less favorable. It is due to the electrostatic repulsion between the adsorptive anion and the surface of the GO that gradually become more negatively charged [64]. Similar phenomena have been reported when $MnFe_2O_4$, $CoFe_2O_4$, Fe_3O_4 nanoparticles, or iron oxide minerals were used to remove Cyanide.

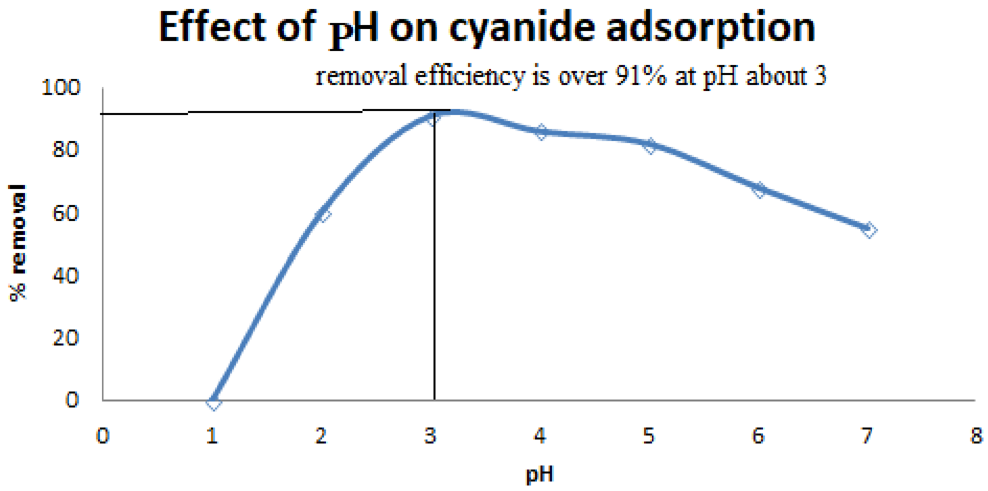

Figure 4.8: pH effect on CN adsorption. (C_o= 20 mg/L, time= 30 min., T=25^{O}C, adsorbent dose= 0.05 g, sol. Volume= 20 mL).

4.2.2 Temperature Effect on Cyanide Adsorption

The effect of temperature on the sorption of CN by Magnetic $CoFe_2O_4$ Graphene Oxide Nanohybride (MGONH) was studied at different temp (15, 25, 35, 45 ◦C) was also studied (Fig.4.9). The results were presented in Figure 4-9. The adjacent shape shows that the absorption process is more suitable at 15 oC temperature. This is mainly due to low surface activity suggesting that the absorption between CN-ion and GO is a thermal reaction. With increasing temperature, attractive forces between the surface of graphene oxide and CN- are weakened and then sorption decreases. Sen et al. [55] has also obtained similar type’s result for a different adsorbent system.

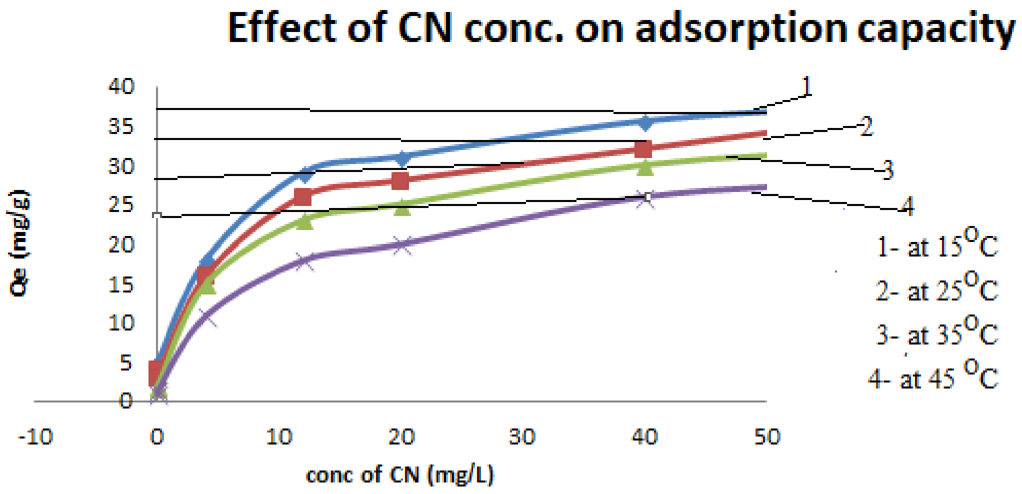

Figure 4.9: Influence of temperature on CN adsorption. (C_o= 20 Mg/L, time= 25 min., adsorbent dose= 0.1 g, sol. Volume= 50 mL)

4.2.3 Effect of contact time

The amount of cyanide adsorbed (qt) at different contact times(5 -60 min). To determine the time of maximum adsorption, the adsorption of CN on Magnetic $CoFe_2O_4$ Graphene Oxide Nanohybride (MGONH) is conducted like a function of contact time as revealed in diagram 4.10.

The adsorption of CN on (MGONH) samples were very fast in the first 5 to 20 min and reached 91%.The adsorption rate becomes almost insignificant after that, because of use of the adsorption sites. The adsorption capacity rate is high at the beginning due to large surface area of adsorbent available for adsorption of cyanide. This is due to the fact that the adsorption process of all interaction sites is vacant at the beginning of the reaction, so the degree of removal is high. After initial rapid absorption, the absorption rate was very slow and almost reached a constant value [65].In our study we used 25 min as a contact time when we studied pH, dose effect etc.

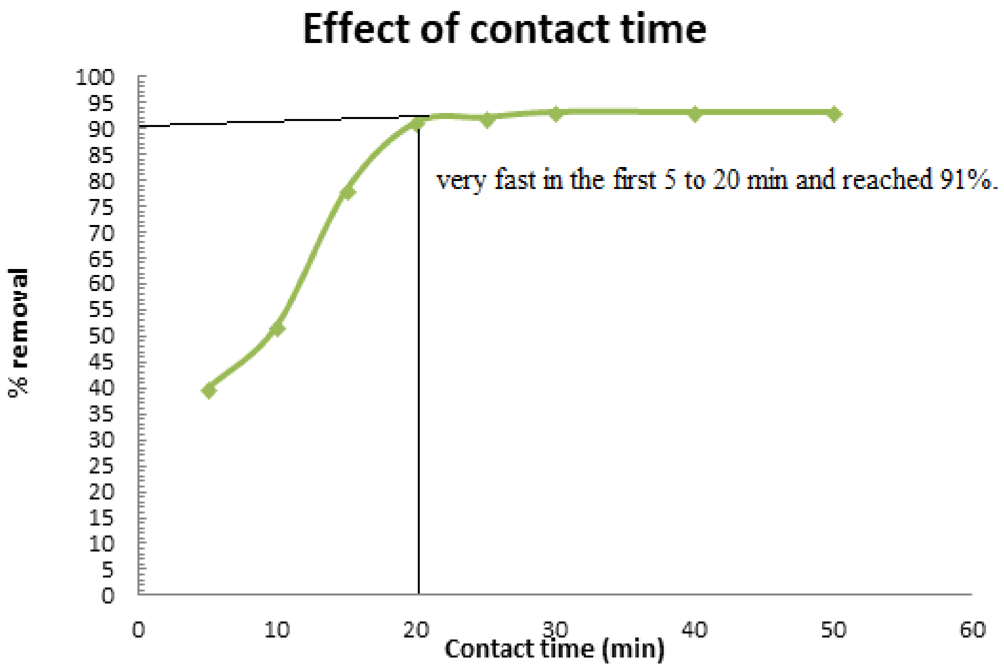

Figure 4.10: Effect of contact time to determine the time of maximum adsorption of CN. (Temp.= 15^{o}C, pH= 3, conc. Of CN= 15 mg/L, sol. Volume= 50 mL, adsorbent dose= 0.2504 g)

4.2.4 Effect of amount of adsorbent

To study the effect of dose of adsorbent on the removal of Cyanide on the Magnetic $CoFe_2O_4$ Graphene Oxide Nanohybride (MGONH) different experiment were done using different dose of (MGONH) substrates ranging between 5 – 600 mg as shown in Fig.4.11. Initial concentration of cyanide solution was preserved at 15 mg/L, initial volume was 20 mL, pH was 3 and temperature was 15C. The results showed in Figure 4.11 that removal efficiency increased significantly with an increase in the dose of adsorbents up to 100mg. There was no marked sign of change in removal efficiency with increased dose of adsorbents. It show that removal efficiency was 91% when the dose was 100mg. For 200m g, it was 91% and 91% for 400mg.

The removal efficiency (% Removal) was calculated using the equation [53].

$$Removal\ efficiency(\%) = \left[\frac{(C_o - C_f)}{C_o}\right] \times 100 \qquad (4.1)$$

Where, Co is the concentration of Cyanide in the sample solution treatment and Ce is the concentration of Cyanide in the sample solution before after treatment.

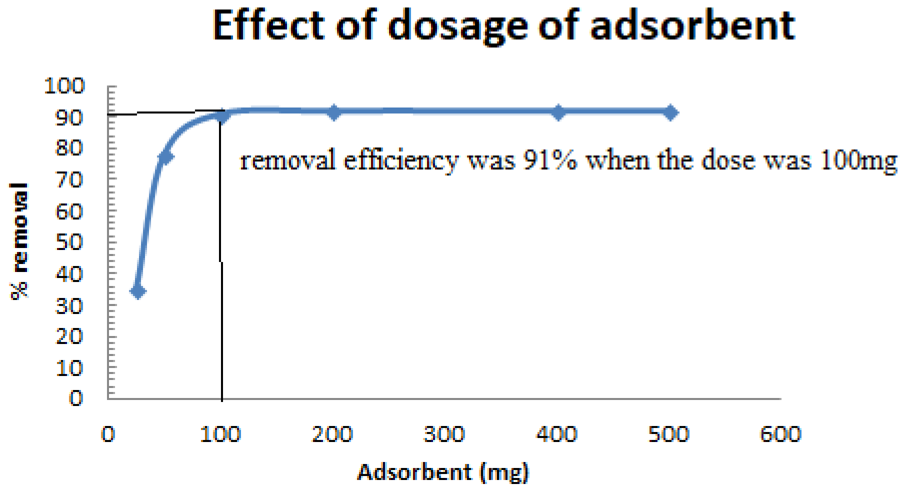

Figure 4.11: Effect of dosage of adsorbent on the removal of CN. (Temp.= 25°C, time= 25 min., pH= 3, conc. of CN= 15 mg/L, sol. Volume= 20 mL)

4.2.5 Influence of cyanide concentration

To study the influence of first focus on expulsion efficiency of Magnetic $CoFe_2O_4$ Graphene Oxide Nanohybride (MGONH) is investigated over wide range of CN concentration keeping other conditions as adsorbent dose, volume of solution and solution pH as constant.

The results are presented in Figure 4.12 It can be noticed from this Figure that uptake of CN was rapid at lower concentration (0.1-1.5 mg/L) and as concentration increase the amount of CN adsorbed was decreased. At lower concentration, the ratio of the initial number of CN molecules to the available surface area is low and the available sites are high, but at high concentrations of CN, the available sites are fewer [66]. Proportion removal of CN lowered from 98% to 76.2%.

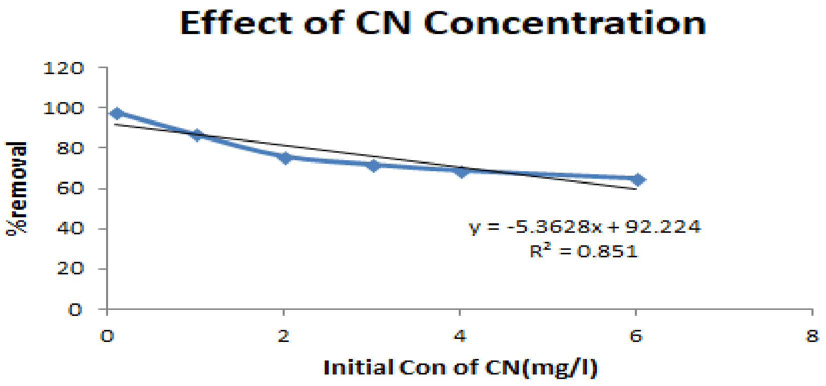

Figure 4.12: Effect of CN concentration on adsorption. (Temp.= 15°C, time= 25 min., pH= 3, adsorbent dose= 0.1 g, sol. Volume= 20 mL).

4.3 Adsorption Isotherm of Cyanide

4.3.1 Langmuir Adsorption Isotherm

Langmuir is based on the kinetic principle and represents adsorption of a monolayer surface on a solid with specific sites strongly identical. [35].

According to equation (2.1), the values of Qm and KL are worked out from slope and the y-intercept of Langmuir plot Ce/Qe opposite, From Langmuir plots which is shown in Figure 4.13 amount adsorbed for monolayer formation (Qm), Langmuir adsorption-desorption equilibrium constant (KL) and regression constant (R2) were determined and values are shown in Table 4.1.

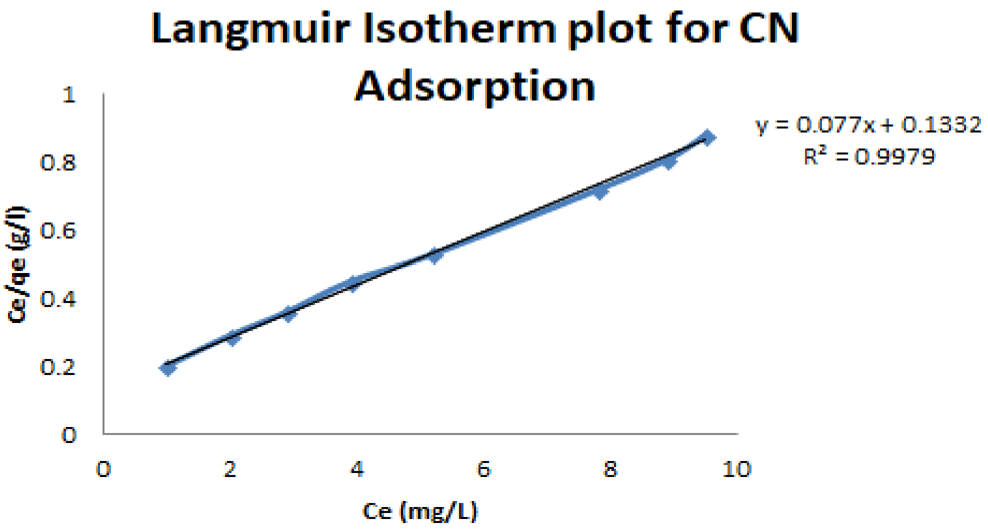

Figure 4.13: Langmuir plot for CN adsorption on (M-Cofe$_2$O$_4$ / GO). (Temp.= 15^{o}C, pH= 3, time= 25 min., sol. Volume= 20 mL, adsorbent dose= 0.1 g)

Table 4.1: Parameters and correlation coefficient of Langmuir isotherm model for adsorption of CN onto (MGONH).

Langmuir isotherm model parameters				
Adsorbate	Parameters			
	Q$_m$ (mg/g)	K$_L$= (L/mg)	R$_L$	R$_2$
(M-Cofe$_2$O$_4$ /	12.98	0.58	0.063	0.9979

The RL value in this investigation was calculated according to equation (2.2). It was found to be equal 0.063 at 15 ◦C which is between 0 and 1 indicating that the CN adsorption on (M-Cofe$_2$O$_4$ / GO) is favorable.

4.3.2Freundlich Adsorption Isotherm

The adsorption to the site of supporting surface surfaces depends on various relationship or the surface of heterogeneous, Freundllich model includes interaction between the adsorbed molecules and represents the non- ideal adsorption that includes heterogeneous surface energy system and reported in Eq. 4.16

$$q_e = K_F C_e^{1/n} \tag{4.1}$$

The linear form of this equation can be written as:

$$\ln q_e = \ln K_F + \frac{1}{n} \ln C_e \tag{4.2}$$

The constants KF (L /mg) and 1/n is the adsorption intensity, were determined by using equation (4.1) which can be used to make a graph of ln(Qe) vs. ln(Ce) as shown in Figure 4.14:

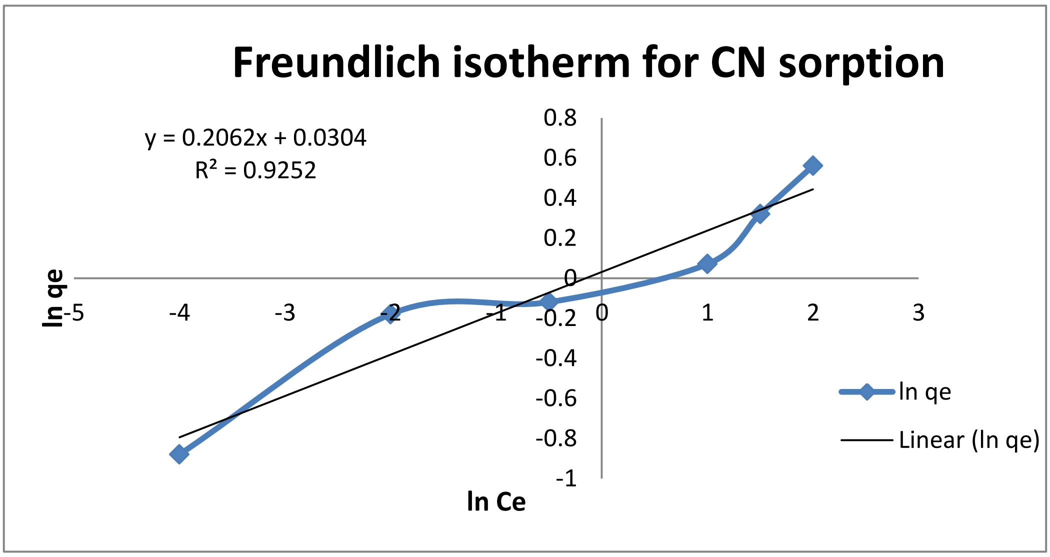

Figure 4.14: Freundlich plot for CN adsorption on (M-Cofe$_2$O$_4$ / GO). (Temp.= 15^{o}C, pH= 3, time= 25 min., sol. Volume= 20 mL, adsorbent dose= 0.1 g).

Freundlich constants K_F and n and regression constant (R_2) were determined and values are shown in Table 4.2:

Table4.2: Parameters and correlation coefficient of Freundlich isotherm model for adsorption of CN onto (M-Cofe$_2$O$_4$ / GO).

Freundlich isotherm model parameters				
Adsorbate Adsorbate	Parameters			
	1/n	**N**	**K_F**	**R^2**
(M-Cofe$_2$O$_4$ / GO)	0.2062	4.8	1.03	0.9252

From the data in Table 4.2, that value of 1/n =0.2062 while n= 4.8 indicating that the sorption of CN on (M-Cofe$_2$O$_4$ / GO) is favorable and the R_2 value is 0.9252 .

The graphically calculated Q_m, K_L, R_L and R_2 (Langmuir isotherm), 1/n, n, K_F, and R_2 (Freundlich isotherm), are rearranged in Table 4.3.

Table4.3:Parameters and correlation coefficient of CN absorption on (M-Cofe$_2$O$_4$ / GO) through Langmuir, Freundlich isotherm model.

Langmuir isotherm model parameters				
	Parameters			
Adsorbate	Q_m (mg/g)	K_L=	R_L	R_2
(M-Cofe$_2$O$_4$ / GO)	12.98	0.58	0.063	0.9979
Freundlich isotherm model parameters				
Adsorbate	Parameters			
	1/n	N	K_F (mg/g (L/mg)1/n)	R_2
(M-Cofe$_2$O$_4$ / GO)	0.2062	4.8	1.03	0.9252

4.4 Adsorption Thermodynamics

To study the behavior of thermodynamics for cyanide absorption using M-Cofe$_2$O$_4$ / GO, through thermodynamic symbols such as the equilibrium constant (K) (L / g), the standard energy of the standard Gibbs energy (ΔG0) (J / mol), the standard entropy (ΔS0) (J / mol.K), standard thermal content (ΔH0) (J / mol) using different temperatures of T (K) and gas constant R (J / K.mol).

There are several equations used to calculate thermodynamics (Eq.4.3and 4.4) [39, 53].

$$\Delta G^0 = \Delta H^0 - T\,\Delta S^0 \qquad (4.3)$$

$$\ln K_d = \frac{\Delta S}{R} - \frac{\Delta H}{RT} \qquad (4.4)$$

ΔH and ΔS can be determined by using from (Figure 4.15), according to equation (4.4):

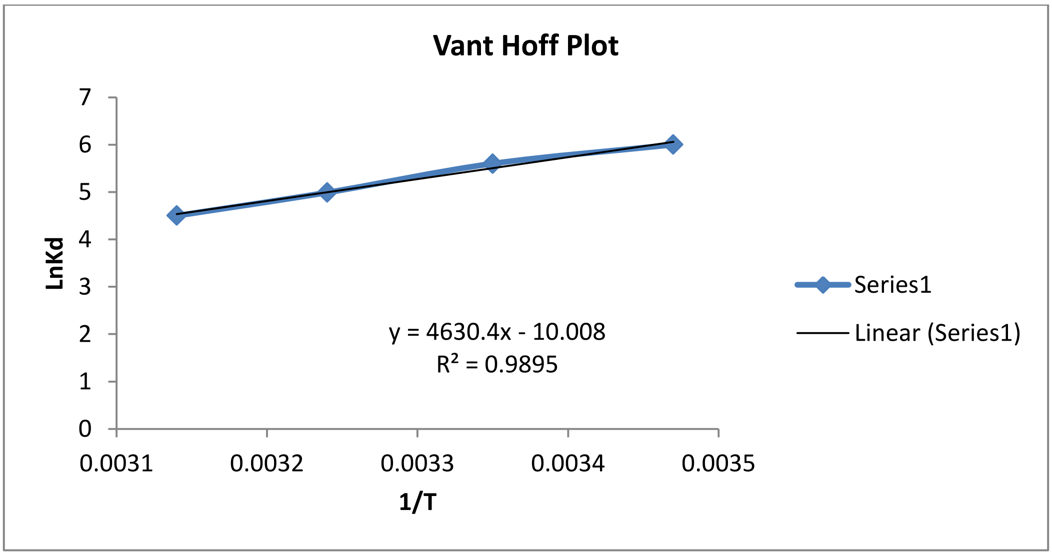

Figure 4.15: drawing of lnKd versus 1/T for CN adsorption on (M-Cofe$_2$O$_4$ / GO). (Temperature= 15°C, pH= 3, time= 25 min., solution Volume= 20 mL, adsorbent dose= 0.1 g).

From the figure to lnKd vs. 1 / T (Fig. 4.15) the values of thermodynamics are calculated from the slope and the y-intercept. Values are shown in Table 4.4. From this table, ΔS^0 value is positive indicating that entropy increases on the surface / solid solution through the absorption process, And The negative ΔH° denotes that this adsorption is an exothermic process, It is clear from the table that all values the Gibbs free energies (ΔG0) were negative and this shows the spontaneous nature of the adsorption process to different temp.

Table 4.4: Thermodynamic data for cyanide absorption for different temperatures.

Adsorbent	ΔH^o(KJ/mol)	ΔS^o(J/mol.K)	ΔG^o (KJ/mol)			
			288 K	298 K	308 K	318K K
(M-Cofe$_2$O$_4$)	-38.493	83.14	-14.548	-13.717	-12.855	-12.596

4.5 Adsorption kinetics of Cyanide

The adsorption kinetics of cyanide on the magnetic graphene samples were studied, The dynamic experimental data were fitted for the first pseudo and the second pseudo order and final the intraparticle propagation model using the following equations (4.5 -4.7):

The pseudo-first ordere equation is:

$$\ln(q_e - q_t) = \ln q_e - K_1 t \qquad (4.5)$$

The pseudo second-order equation is:

$$\frac{t}{q_t} = \frac{1}{q_e}t + \frac{1}{K_2 q_e^2} \qquad (4.6)$$

The intraparticle diffusion model equation is

$$q_t = K_{id}t^{1/2} + Z \qquad (4.7)$$

where q_t and q_e are adsorption capacities (mg/g) at balance and different period (min), sequenially, K_1 is the first pseudo order average stability (min-1), K_2 is the second pseudo order average stability (g /mg.min). The K_{id} is the intraparticle diffusion average stability (mg/ g.min$^{1/2}$) and Z (mg/ g) which gives information about the thickness of boundary layer [42].

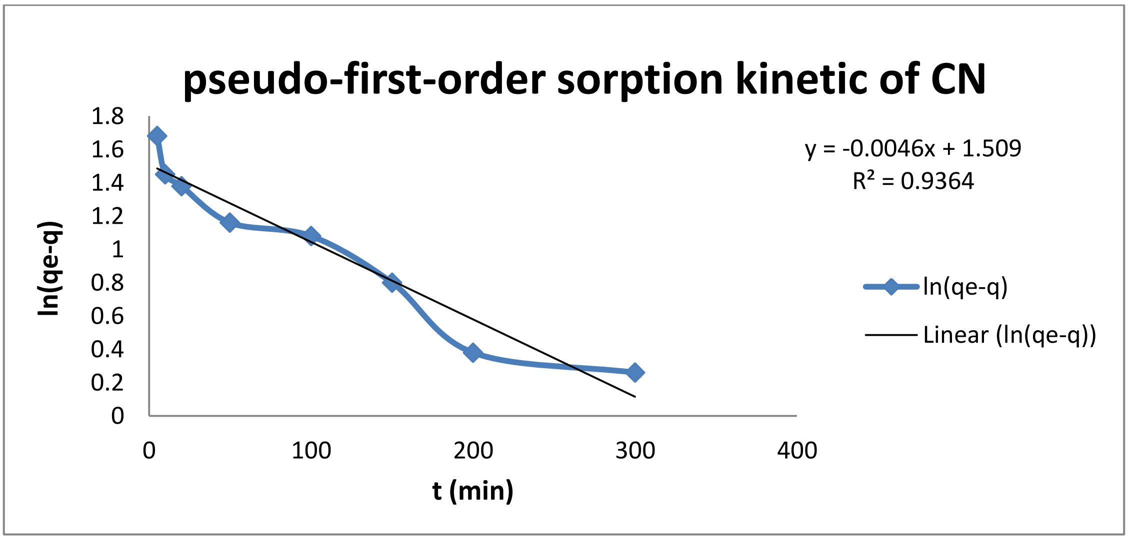

Figure 4.16: Drawing Pseudo first order sorption kinetics of CN on M-Cofe$_2$O$_4$ / GO. (Temperature= 15°C, pH= 3, solution Volume= 50 mL, adsorbent dose= 0.1 g).

Table 4.5: Pseudo first order parameters for CN adsorption onto M-Cofe$_2$O$_4$ / GO 15C.

Adsorbent	Qe (exp mg/g)	Pseudo first order		
		K1 (mi n^{-1})	Qe (calc) (mg/g)	R^2
M-Cofe$_2$O$_4$ / GO	36.4	4.6×10^{-4}	4.1	0.9364

The experimental Q_e value does not match with the calculated Q_e value (Table 4.6). This pointed that the adsorption of CN does not obey the first-order kinetics so that the pseudo first order model is not the appropriate one [67].

Through Figure 4.16, the results confirm that the second-order binary dynamic model is fully consistent with the experimental data with the linear regression coefficient of 0.9979.

The correlation coefficients (R_2) for the pseudo second order was higher than the pseudo-first-order and it reached 0.9979 in most of the samples.

Q_e experimental and Q_e calculated values for the pseudo second order model are illustrated in Table 4.5. It can be observed from this table that there is an agreement between Q_e experimental and Q_e calculated values for the pseudo second order model. Also K_2 is much greater than K_1. Hence, the pseudo second order model well represented the adsorption kinetics.

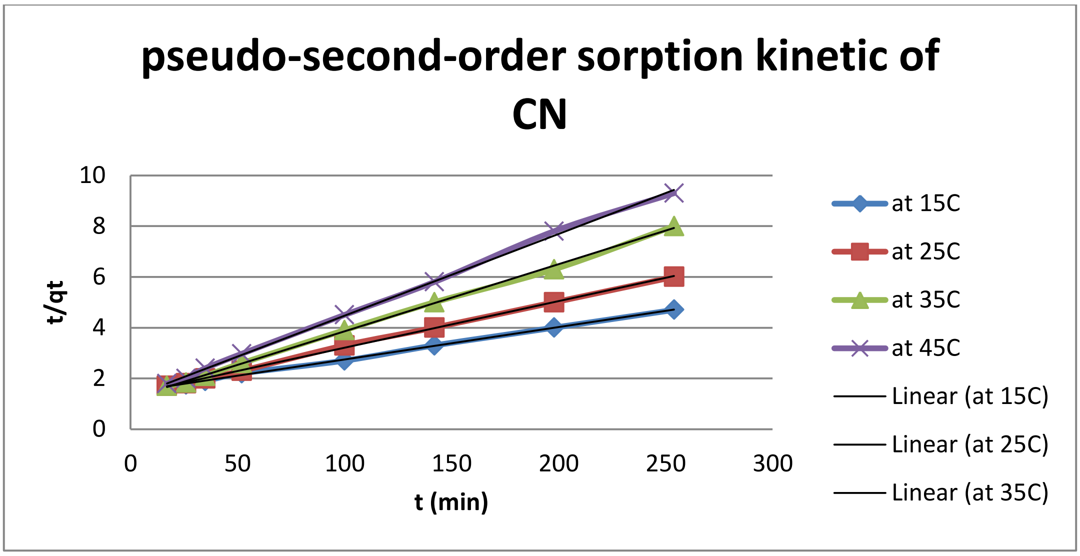

Figure 4.17: drawing Pseudo second order adsorption kinetics of CN on M-Cofe$_2$O$_4$ / GO. (pH= 3, solution Volume= 50 mL, adsorbent dose= 0.1 g).

Table 4.6: pseudo second order parameters for CN adsorption onto M-Cofe$_2$O$_4$ / GO 4 at different temp^{O}C.

Temp	q_e (exp) (mg/g)	Pseudo-second -order		
		K_2 (g/(mg.min))	q_{cal}(mg/g)	R^2
15 $^{O}{}_{c}$	37.4	$5.5 * 10^{-4}$	37.09	0.9999
25$^{O}{}_{c}$	34.6	$3.5 * 10^{-3}$	33.8	0.9999
35 $^{O}{}_{c}$	27.8	$6.8 * 10^{-3}$	26.2	0.9998
45 $^{O}{}_{c}$	24.3	$8.8 * 10^{-3}$	23.8	0.9997

The Weber–Morris methodl was utillized to achieve if intraparticle diffusion was the rate-controlling step of this adsorption using Equation:

$$\mathbf{qt = K_d\, t_{1/2} + z} \qquad (4.8)$$

Where z (mg/g) is a constant associated with thickness boundary layer and Kd is intraparticle diffusion average stability mg/(g/min1/2)[67]. When drawing of qt against t1/2 which passes through the origin indicates intraparticle diffusion as the major rate-controlling step. However, From the Figure 4.18 show which does not pass through the origin indicating that the rate limiting process is not the only rate-limiting step . The intraparticle diffusion plot of this study, as shown in Figure 4.18, shows a linear plot which deviates from the origin, thus intraparticle controlling the rate of cyanide adsorption on M-Cofe$_2$O$_4$ / GO diffusion is involved but.

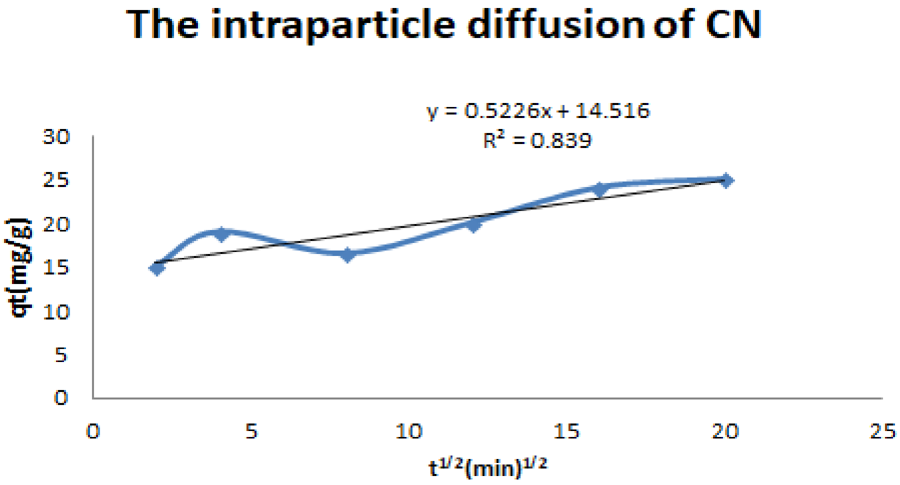

Figure 4.18: The intraparticle diffusion of CN on M-Cofe$_2$O$_4$ / GO. (Temperature= 15^{o}C, pH= 3, solution Volume= 50 mL, adsorbent dose= 0.1 g).

Intraparticle diffusion model	
K$_{id}$	Z
0.5226	14,516

4.6 Recovery and reusability of M-Cofe$_2$O$_4$ / GO adsorbent

To achieved see how many times we can use the adsorbents and see their efficiencies, this part of experiment is done. The experiment is repeated 4 times using the same adsorbent, so the results are shown in Table 4.7. Recovering CN from M-Cofe$_2$O$_4$ / GO was carried out at 15 ◦C. The adsorbent was recovered by filtration, washed with portions of 6N HCl and then washed with deionized water and drought at room temperature for two days. Under similar conditions, the adsorption capability of regenerated M-Cofe$_2$O$_4$ / GO is tested and compared to the first use.

Table 4.7: Recovering CN from M-Cofe$_2$O$_4$ / GO was carried out at 15 ◦C.

Recycling times	1	2	3
Removal efficiencies of Cyanide, %)	91	90.2	89.3

Conclusions

Cyanide adsorption efficiency of M-Cofe$_2$O$_4$ / GO was investigated in this study.

Depending on the results, (M-Cofe$_2$O$_4$ / GO) was able to remove CN rapidly within 25 min with low removal efficiency 91% at pH 3, 15^{O}C temperature, 0.25 g weight of dose and initial concentration of 15 mg/L of 50mL cyanide solution. around 91% removal efficiency of Cyanide was achieved after 25 min. at the same condition.

The adsorption isotherm conformed was predicted to follow Langmuir isotherm model. The kinetics follow the pseudo-second-order reaction model, which for the most part denotes a case of chemisorption as the mechanism of adsorption. When the correlation coefficients (R^2) for the pseudo second order was higher than that for the pseudo-first-order and it reached 0.9999 for the samples. The calculated q_e values for the pseudo-second-order were very close to the experimental q_e values indicating that the adsorption process of CN on the surfaces of graphene magnetic were followed and described by the pseudo-second-order.

The results of this study indicate the ΔS^0 values were positive for the adsorption process, indicating that the surface / solution was randomized during the absorption process, while ΔH^0 values were negative for M-Cofe$_2$O$_4$ / GO particles due to their exothermic nature. The free energies of M-Cofe$_2$O$_4$ / GO were negative, indicating the spontaneous nature of adsorption at different temperatures.

M-Cofe$_2$O$_4$ / GO is a good effective pipette to remove cyanide from wastewater. M-Cofe$_2$O$_4$ / GO has a low absorption capacity compared to many other non-conventional adsorbents. M-Cofe$_2$O$_4$ / GO can provide an appropriate method for effective treatment of industrial wastewater contaminated with under acidic cyanide, and a low concentration of CN at a temperature of about 15 ° C to remove more than 70%.

.

References

[1] S. Sirianuntapiboon, C. Chuamkaew, **Packed cage rotating biological contactor system for treatment of cyanide wastewater**, Bioresour. Technol. 98 (2007) 266–272.

[2] Rajappa A., Ramesh K., Nandhakumar V., Ramesh H., Sivakumar S., Savithri S. 2014 August 27, ***Thermodynamics and Instrumental Analysis of Congo Red Dye Adsorption onto Commercial Activated Carbon***, **International Journal of Chemistry and Pharmaceutical Sciences**, Vol. 2 (8): 1068-1073.

[3] A.Y. Dursun, A. C¸ alik, Z. Aksu, **Degradation of ferrous(II) cyanide complex ions by Pseudomonas fluorescens**, Process Biochemistry, Volume 34, Issue 9, October 1999, Pages 901-908.

[4] M.G. Campos, P. Pereira, J.C. Roseiro, **Packed-bed reactor for the integrated biodegradation of cyanide and formamide by immobilised Fusarium oxysporum CCMI 876 and Methylobacterium sp**. RXM CCMI 908, Enzyme Microb. Technol. 38 (2006) 848–854.

[5] M. Habuda-Stanić, M. Nujić, **Arsenic removal by nanoparticles: a review, Environmental Science and Pollution Research**, 22 (2015) 8094-8123.

[6] R.R. Dash, C. Balomajumder, A. Kumar, ***Removal of cyanide from water and wastewater using granular activated carbon,*** **Chem. Eng. J.** 146 (2009) 408–413.

[7] Rashed N., **Adsorption Technique for the Removal of Organic Pollutants from Water and Wastewater**, InTech; Organic Pollutants - Monitoring, Risk and Treatment; 2013; Ch.7 167-193;Available from: http://dx.doi.org/10.5772/54048.

[8] Czelej K., Cwieka K., Colmenares J.C., Kurzydlowski K.J. **Insight on the Interaction of Methanol-Selective Oxidation Intermediates with Au- or/and Pd-Containing Monometallic and Bimetallic Core@Shell Catalysts**, Langmuir 2016 32 (30), p. 7493-7502.

[9] Dada A., Olalekan A., Olatunya A., DADA O., 2012 Nov. – Dec, ***Langmuir, Freundlich, Temkin and Dubinin – Radushkevich Isotherms Studies of Equilibrium Sorption of Zn2+ Unto Phosphoric Acid Modified Rice Husk***, **IOSR Journal of Applied Chemistry**, Vol. 3 (1): 38-45.

[10] Y. Shen, B. Chen, **Sulfonated graphene nanosheets as a superb adsorbent for various environmental pollutants in water,** Environ. Sci. Technol. 49 (2015) 7364–7372.

[11] X. Ren, J. Shi, L. Tong, Q. Li, H. Yang, **Magnetic and luminescence properties of the porous CoFe2O4@Y2O3: Eu3+ nanocomposite with higher coercivity, J. Nanopart.** Res. 15 (2013) 1738

[12] C.A. Young, T.S. Jordan, **Cyanide remediation: current and past technologies**, in: Proceedings of the 10th Annual Conference on Hazardous Waste Research, 1995, pp. 104–129.

[13] S. Chella, P. Kollu, E.V.P. Komarala, S. Doshi, M. Saranya, S. Felix, R. Ramachandran, P. Saravanan, V.L. Koneru, V. **Venugopal**, **Solvothermal synthesis of MnFe2O4-graphene composite—Investigation of its adsorption and antimicrobial properties**, Appl. Surf. Sci. 327 (2015) 27–36.

[14] Agency for Toxic Substances and Disease Registry (ATSDR). **Toxicological Profile for Cyanide (Update).** Public Health Service, U.S. Department of Health and Human Services, Atlanta, GA. 1997.

[15] Oliveira, G. E.a*, Clarindo, J. E. S.a, Santo, K. S. E.a, Souza Jr., F. G.b, **Chemical Modification of Cobalt Ferrite Nanoparticles with Possible Application as Asphaltene Flocculant Received**: October 31, 2012; Revised: February 15, 2013.

[16] Y. Yao, S. Miao, S. Liu, L.P. Ma, H. Sun, S. Wang, ***Synthesis**, **characterization, and adsorption properties of magnetic Fe3O4@graphene nanocomposite, Chem.*** **Eng. J.** 184 (2012) 326–332.

[17] A. Zheng, D.A. Dzombak, R.G. Luthy, B. Sawer, W. Lazouska, P. Tata, M.F. Delaney,LZilitinkevitch, J.R. Sebriski, R.S. Swartling, S.M. Drop, J.M. Flaherty, **Evaluation and testing of analytical methods for cyanide species in municipal and industrial contaminated water**, Environ. Sci. Technol. 37 (2003) 107–115.

[18] Sharifi, T. et al. **Nitrogen doped multi walled carbon nanotubes produced by CVD-correlating XPS and Raman spectroscopy for the study of nitrogen inclusion**. Carbon. N. Y. 50, 3535–3541 (2012).

[19] C. Su, R.W. Puls, **Arsenate and Arsenite Removal by Zerovalent Iron: Kinetics, Redox Transformation, and Implications for in Situ Groundwater Remediation**, Environ. Sci. Technol., 35 (2001) 1487-1492.

[20]X. Ren, J. Shi, L. Tong, Q. Li, H. Yang, ***Magnetic and luminescence properties of the porous CoFe2O4@Y2O3: Eu3+ nanocomposite with higher coercivity***, **J. Nanopart.** Res. 15 (2013) 1738.

[21] C.A. Young, T.S. Jordan, **Cyanide remediation: current and past technologies,** in: Proceedings of the 10th Annual Conference on Hazardous Waste Research, 1995, pp. 104–129.

[22] R.R. Dash, C. Balomajumder, A. Kumar, ***Removal of cyanide from water and wastewater using granular activated carbon, Chem.*** **Eng. J.** 146 (2009) 408–413.

[23] Rashed N., **Adsorption Technique for the Removal of Organic Pollutants from Water and Wastewater**, InTech; Organic Pollutants - Monitoring, Risk and Treatment; 2013; Ch.7 167-193;Available from: http://dx.doi.org/10.5772/54048.

[24] S. Kumar, R.R. Nair, P.B. Pillai, S.N. Gupta, M.A.R. Iyengar, A.K. Sood, **Graphene oxide–MnFe2O4 magnetic nanohybrids for efficient removal of lead and arsenic from water**, ACS Appl. Mater. Interfaces 6 (2014) 17426– 17436.

[25] M.M. Botz, ***Overview of cyanide treatment methods, in: Mining Environmental Management,*** **Mining Journal Ltd.,** London, UK, 2001, pp. 28–30.

[26] Ewa Jaszczak,corresponding author Żaneta Polkowska, Sylwia Narkowicz, and Jacek Namieśnik, **Cyanides in the environment—analysis—problems and challenges**. Environ Sci Pollut Res Int. 2017; 24(19): 15929–15948.

[27] Akinsola R. Omotayo, Abubakar EL-Ishaq*, Alade S. Babatunde ***Assessment of Cyanide Content in White, Light Yellow and Deep Yellow Cassava Grit (Gari) Sold in Damaturu Metropolis***. **American Journal of Food Science and Health**, Vol. 1, No. 5, 2015, pp. 109-113 .

[28] UNEP, Desk Study on the Environment in the Occupied Palestinian Territories, March 2001, 42-87.

[29] Y. Zhang, B. Chen, L. Zhang, J. Huang, F. Chen, Z. Yang, J. Yao, Z. Zhang, **Controlled assembly of Fe3O4 magnetic nanoparticles on graphene oxide,** Nanoscale 3 (2011) 1446–1450.

[30] S. Zhang, H. Niu, Y. Cai, X. Zhao, Y. Shi, ***Arsenite and arsenate adsorption on coprecipitated bimetal oxide magnetic nanomaterials: MnFe2O4 and CoFe2O4,*** **Chem. Eng. J**., 158 (2010) 599-607.

[31] Czelej K., Cwieka K., Colmenares J.C., Kurzydlowski K.J. **Insight on the Interaction of Methanol-Selective Oxidation Intermediates with Au- or/and Pd-Containing Monometallic and Bimetallic Core@Shell Catalysts**, Langmuir 2016 32 (30), p. 7493-7502.

[32] Rashed N., **Adsorption Technique for the Removal of Organic Pollutants from Water and Wastewater, InTech; Organic Pollutants - Monitoring, Risk and Treatment**; 2013; Ch.7 167-193;Available from: http://dx.doi.org/10.5772/54048.

[33] Worch E., **Adsorption Technology in Water Treatment-Fundamentals, Processes, and Modeling, Germany**, Walter de Gruyter GmbH & Co. KG, 2012, 345 p.

[34] Ferraria L., Kaufmann J., Winnefeld F., Plank J. July 2010, ***Interaction of cement model systems with superplasticizers investigated by atomic force microscopy, zeta potential, and adsorption measurements***, **J Colloid Interface Sci**., Vol. 347 (1): 15–24.

[35] Mehdi Vadi, et al (2014), Langmuir, ***Freundlich and Temkin Adsorption Isotherms of Propranolol on Multi-Wall Carbon Nanotube***. **J. of Modern Drug Discovery and Drug Delivery Research**. V1I3. DOI: 10.15297/JMDDR.V1I3.01.

[36] Malek A., Farooq S., 1996 Nov., ***Comparison of isotherm models for hydrocarbon adsorption on activated carbon***, **AIChE J**., Vol. 42 (11): 3191–3201.

[37] Foo K., Hameed B., 2009 Sep. 7, ***Insights into the modeling of adsorption isotherm systems,*** **Chemical Engineering J**., 156: 2–10.

[38] Dogan, M., Alkan, M., J. **Colloid Interface Sci**., 267 (2003) 32.

[39] Dada A., Olalekan A., Olatunya A., DADA O., 2012 Nov. – Dec, Langmuir, ***Freundlich, Temkin and Dubinin – Radushkevich Isotherms Studies of Equilibrium Sorption of Zn2+ Unto Phosphoric Acid Modified Rice Husk***, **IOSR Journal of Applied Chemistry**, Vol. 3 (1): 38-45.

[40] M.M. Botz, ***Overview of cyanide treatment methods, in: Mining Environmental Management,*** **Mining Journal Ltd., London, UK**, 2001, pp. 28–30.

[41] Hall, K. R., Eagleton, L. C., Acrivers, A., Vermenlem, T., Ind. **Eng. Chem**. Res., 5 (1966) 212.

[42] Hisham J. El-Aila *, Khaled M. Elsousy, Khaled A. Hartany Kinetics, **equilibrium, and isotherm of the adsorption of cyanide by MDFSD 2 January 2011**; accepted 3 March 2011.

[43] S. Sirianuntapiboon, C. Chuamkaew, **Packed cage rotating biological contactor system for treatment of cyanide wastewater**, Bioresour. Technol. 98 (2007) 266–272.

[44] S.H. Chien, W.R. Clayton, ***Application of Elovich equation to the kinetics of phosphate release and sorption on soils***, Soil Sci. Soc. **Am. J**. 44 (1980) 265– 268.

[45] B.H. Hameed, I.A.W. Tan, A.L. Ahmad, ***Adsorption isotherm, kinetic modeling and mechanism of 2,4,6-trichlorophenol on coconut husk-based activated carbon***, **Chem. Eng. J**. 144 (2008) 235–244.

[46] A. Benhammou, A. Yaacoubi, L. Nibou, B. Tanouti, ***Adsorption of metal ions onto Moroccan stevensite: kinetic and isotherm studies***, **J. Colloid Interface Sci**. 282 (2005) 320–326.

[47] Hashem, A. and El-Khiraigy, K. (2013) ***Bioadsorption of Pb(II) onto Anethum graveolens from Contaminated Wastewater: Equilibrium and Kinetic Studies***. **Journal of Environmental Protection**, 4, 108-119. http://dx.doi.org/10.4236/jep.2013.41012.

[48] Qiu, H., Lv, L., Pan, B.-C., Zhang, Q.-J., Zhang, W.-M. and Zhang, Q.-X. (2009) ***Critical Review in Adsorption Kinetic Models***. **Journal of Zhejiang University Science** A, 10, 716-724. http://dx.doi.org/10.1631/jzus.A0820524.

[49] Priyantha, N. and Bandaranayaka, A. (2011) ***Investigation of Kinetics of Cr(VI)-Fired Brick Clay Interaction***. **Journal of Hazardous Materials**, 188, 193-197. http://dx.doi.org/10.1016/j.jhazmat.2011.01.090.

[50] Tan I., Hameed B., Ahmad A., 2007 Mar. 1, ***Equilibrium and Kinetic studies on basic dye adsorption by oil palm fiber activated carbon**,* **Chemical Engineering Journal**, Vol. 127(1–3): 111–119.

[51] Olayinka John Akinyeye1, ***Tope Babatunde Ibigbami2, Oluwakayode Odeja3 2016, Effect of Chitosan Powder Prepared from Snail Shells to Remove Lead (II) Ion and Nickel (II) Ion from Aqueous Solution and Its Adsorption Isotherm Model,*** **American Journal of Applied Chemistry**; 4(4): 146-156.

[52] H.DeveciE.Y.YazıcıI.AlpT.Uslu, **Removal of cyanide from aqueous solutions by plain and metal-impregnated granular activated carbons** Volume 79, Issue 3, June 2006, Pages 198-208.

[53] G.holamreza, M.oussavi, R.asoul, K.hosravi ,**Removal of cyanide from wastewater by adsorption onto pistachio hull wastes: Parametric experiments, kinetics and equilibrium analysis** ,Volume 183, Issues 1–3, 15 November 2010, Pages 724-730.

[54] J.M. Salman, F.M. Abid, **Preparation of mesoporous activated carbon from palm-date pits: optimization study on removal of bentazon**, carbofuran, and 2,4-D using response surface methodology, Water Sci. Technol. 68 (2013) 1503–1511.

[55] M. Ghaedi, A. Ansari, M.H. Habibi, A.R. Asghari, ***Removal of malachite green from aqueous solution by zinc oxide nanoparticle loaded on activated carbon***: ***kinetics and isotherm study***, **J. Ind. Eng**. Chem. 20 (2014) 17–28.

[56] M. Eissam, N.Oroozifar, M.Ozhgan, L. KhorasaMotlaghParisaAhmadzadeh Fard, **Cyanide uptake from wastewater by modified natrolite zeolite–iron oxyhydroxide system: Application of isotherm and kinetic models**, Volume 166, Issues 2–3, 30 July 2009, Pages 1060-1066.

[57] F. Li, Y. Wang, Q. Yang, D.G. Evans, C. Forano, X. Duan, ***Study on*** **adsorption** ***of glyphosate (N-phosphonomethyl glycine) pesticide on*** **MgAl-layered** ***double hydroxides in aqueous solution***, **J. Hazard. Mate**r. 125 (2005) 89–95.

[58] A. Martín, A. Escarpa, **Graphene: the cutting–edge interaction between chemistry and electrochemistry**, TrAC, Trends Anal. Chem. 56 (2014) 13–26.

[59] S. Kumar, R.R. Nair, P.B. Pillai, S.N. Gupta, M.A.R. Iyengar, A.K. Sood, **Graphene oxide–MnFe2O4 magnetic nanohybrids for efficient removal of lead and arsenic from water**, ACS Appl. Mater. Interfaces 6 (2014) 17426– 17436.

[60] Shigeru Nagashima , Takejiro Ozawa. ***Spectrophotometric Determination of Cyanide with Isonicotinic Acid and Barbituric Acid,*** **International Journal of Environmental Analytical Chemistry**, Volume 10, 1981 - Issue 2, Published Online: 13 Dec 2006.

[61] Hashem, A. and El-Khiraigy, K. (2013) ***Bioadsorption of Pb (II) onto Anethum graveolens from Contaminated Wastewater: Equilibrium and Kinetic Studies.*** **Journal of Environmental Protection**, 4, 108-119. http://dx.doi.org/10.4236/jep.2013.41012.

[62] S. Zhang, H. Niu, Y. Cai, X. Zhao, Y. Shi, ***Arsenite and arsenate adsorption on coprecipitated bimetal oxide magnetic nanomaterials: MnFe2O4 and CoFe2O4***, **Chem. Eng. J**., 158 (2010) 599-607

[63] Y. Li, Q. Du, T. Liu, J. Sun, Y. Jiao, Y. Xia, L. Xia, Z. Wang, W. Zhang, K. Wang, H. Zhu, D. Wu, **Equilibrium, kinetic and thermodynamic studies on the adsorption of phenol onto graphene,** Materials Research Bulletin 47 (2012) 1898–1904.

[64] Weber, W.J., Jr.; Morris, J.C. ***Kinetics of adsorption on carbon from solution***. **J. Sanit. Eng. Div**. 1963, 89, 31–60.

[65] Hameed, B.H.; Mahmoud, D.K.; Ahmad, A.L. ***Equilibrium modelling and kinetic studies on the adsorption on basic dye by a low cost adsorbent: Coconut (Cocos nucifera) bunch waste.*** **J. Hazard. Mater**. 2008, 158, 65–72. [CrossRef] [PubMed].

[66] S. Zhang, H. Niu, Y. Cai, X. Zhao, Y. Shi, ***Arsenite and arsenate adsorption on coprecipitated bimetal oxide magnetic nanomaterials: MnFe2O4 and CoFe2O4***, **Chem. Eng. J**., 158 (2010) 599-607.

[67] Xinguang Zhou, Yinglu Zhang, Zuteng Huang, Dingkun Lu, **Anwei Zhu & Guoyue Shi Ionic liquids modified graphene oxide composites: a high efficient adsorbent for phthalates from aqueous solution**, Scientific Reports volume 6,

جامعة النجاح الوطنية

كلية الدراسات العليا

فعالية كوبالت أكسيد الحديد $CoFe_2O_4$ المغناطيسي المثبت على الجرافين لإزالة السيانيد من مياه الصرف الصحي

اعداد

أحمد خضر طه زبيده

اشراف

أ.د. شحدة جودة

قدّمت هذه الأطروحة استكمالاً لمتطلبات الحصول على درجة الماجستير في الكيمياء، بكلية الدراسات العليا، في جامعة النجاح الوطنية، نابلس–فلسطين.

2018

فعالية كوبالت أكسيد الحديد $CoFe_2O_4$ المغناطيسي المثبت على الجرافين لإزالة السيانيد من مياه الصرف الصحي

إعداد

أحمد خضر طه زبيده

إشراف

أ.د. شحدة جودة

الملخص

هناك العديد من الملوثات التي تتسرب إلى التربة والمياه الجوفية من دون علاج. فهي تسبب العديد من المشاكل الصحية لكل من البشر والحيوانات. المشكلة الرئيسية هنا هي للكشف عن تركيز الملوثات مثل السيانيد ومحاولة إزالته عن طريق الامتزاز.

تم تشخيص الجرافين المغناطيسي $M\text{-}CoFe_2O_4 - G0$ من خلال عدة تقنيات طيفية وتحليلية، SEM, TEM, XRD, FTIR, VSM, TGA وأظهرت صور المسح الضوئي للمجهر الالكتروني للمغناطيسية طبيعة خشنة ومسامية، مما يشير إلى أن المواد تمثل خصائص جيدة ليتم استخدامها كإدمصاص. وأجريت تجارب الادمصاص لمجموعة واسعة من درجات الحرارة، والجرعات المستخدمة في عملية الإدمصاص، ودرجة الحموضة، والتركيز الأولي، و زمن التفاعل. لوحظ أن التركيز يزيد من كمية السيانيد الممزوج ودرجة الحرارة بينما يزداد مع زيادة الرقم الهيدروجيني للمحلول، وقت التلامس والجرعة الممتزة. تم تحقيق كفاءة إزالة 91٪ من السيانيد بعد 25 دقيقة ، عند درجة الحموضة تساوي 3، و15 درجة مئوية بإستخدام وزن 0،25 غرام من الجرعة والتركيز الأولي 15 مغ / لتر من 50 مل.

تم تحسين ادمصاص السيانيد على الجرافين في الظروف الحمضية ودرجات الحرارة. ويمكن وصف ادمصاص السيانيد باستخدام الجرافين من خلال Pseudo second order and Langmuir isotherm. استناداً إلى النتائج، فإن $M\text{-}CoFe_2O_4 - G0$ قادر على إزالة السانيد بسرعة في غضون 25 دقيقة مع كفاءة إزالة عالية.

تشير قيم الطاقة الحرة السلبية (–14.548 إلى –12.595 كيلو جول / مول) إلى أن الإدمصاص مناسب وتلقائي عند درجات الحرارة هذه. تعكس القيمة السالبة للمحتوى الحراري (–38.9 كيلو جول/ مول) الادمصاص الحراري وتشير إلى أن درجة الادمصاص هي 15ْ م. وكانت قيمة المحتوى الحراري أعلى من تلك المقابلة للادمصاص المادي. هذا من شأنه أن يشير إلى أن عملية الادمصاص هي مادة كيميائية في طبيعتها. تشير القيمة الإيجابية للفوضى (+83.14 جول/ مول. كلفن) إلى بعض التغييرات الهيكلية على الممتزات وزيادة العشوائية الصلبة / السائلة في نظام الامتصاص أثناء الامتصاص